QBOi El Niño–Southern Oscillation experiments: Teleconnections of the QBO

Naoe, Hiroaki[1], Jorge L. García-Franco[2], Chang-Hyun Park[3], Mario Rodrigo[4], Froila M. Palmeiro[4,5], Federico Serva[6], Masakazu Taguchi[7], Kohei Yoshida[1], James A. Anstey[8], Javier García-Serrano[4,9], Seok-Woo Son[3], Yoshio Kawatani[10], Neal Butchart[11], Kevin Hamilton[12], Chih-Chieh Chen[13], Anne Glanville[13], Tobias Kerzenmacher[14], François Lott[15], Clara Orbe[16], Scott Osprey[17], Mijeong Park[13], Jadwiga H. Richter[13], Stefan Versick[14], Shingo Watanabe[18, 19]

[1]Meteorological Research Institute (MRI), Tsukuba, 305-0052, Japan
[2]National School of Earth Sciences (Escuela Nacional de Ciencias de la Tierra), UNAM, CDMX, 04510, Mexico
[3]School of Earth and Environmental Sciences, Seoul National University, Seoul, 08826, Korea
[4]Group of Meteorology, Universitat de Barcelona, Barcelona, 08028, Spain
[5]CMCC Foundation - Euro-Mediterranean Center on Climate Change, Bologna, 40127, Italy
[6]Institute of Marine Sciences, National Research Council (CNR-ISMAR), 00133, Italy
[7]Department of Earth Science, Aichi University of Education, Kariya, 448-0001, Japan
[8]Canadian Centre for Climate Modelling and Analysis, Environment and Climate Change Canada, V8N 1V8, Canada
[9]Barcelona Supercomputing Center (BSC), Barcelona, 08034, Spain
[10]Faculty of Environmental Earth Science, Hokkaido University, Sapporo, 060-0810, Japan
[11]Met Office, Exeter, EX1 3PB, UK
[12]International Pacific Research Center (IPCC) University of Hawaii, Honolulu, 96822, USA
[13]U. S. National Science Foundation National Center for Atmospheric Research (NSF NCAR), Boulder, 80305, USA
[14]Karlsruher Institut für Technologie (KIT), Karlsruhe, 76131, Germany
[15]Laboratoire de Météorologie Dynamique (LMD), Ecole Normale Supérieure, Paris, 75231, France
[16]National Aeronautics and Space Administration (NASA) Goddard Institute for Space Studies (GISS), New York, 10025, USA
[17]Atmospheric, Oceanic and Planetary Physics, University of Oxford, Oxford, OX1 3PU, UK
[18]Japan Agency for Marine-Earth Science and Technology (JAMSTEC), Yokohama, 236-0001, Japan
[19]Advanced Institute for Marine Ecosystem Change, Tohoku University, Sendai, 980-8578, Japan

Correspondence to: Hiroaki Naoe (hnaoe@mri-jma.go.jp)

September~~August~~, 2025

Revised, to be submitted to Weather and Climate Dynamics

Abstract. This study investigates~~examines~~ Quasi-Biennial Oscillation (QBO) teleconnections and their modulation by the El Niño–Southern Oscillation (ENSO)~~,~~ using a multi-model ensemble from~~of~~ the Atmospheric Processes And their Role in Climate (APARC) QBO initiative (QBOi)~~ models~~. ~~Some difficulties arise in ~~Analyzing~~examining~~ observed QBO–ENSO

teleconnections is challenging because it is difficult tofrom separatedistinguishing the respective influences of QBO and ENSO influences outside of the QBO region, due to aliasing between the QBO and ENSO overin the historical record. To isolateseparate thesethe QBO and ENSO signals, simulations awere conducted with annually -repeating prescribed sea-surface temperatures representingcorresponding to idealized El Niño andor La Niña conditions (the QBOi EN and LN experiments, respectively). In LN, four out of nine models are to reproduce the observed Holton-TanHolton–Tan relationship within a half of the observed amplitude. In the Arctic winter climate, higher frequencies of sudden stratospheric warmings (SSWs) occur more frequentlyare found in EN than in LN;, however,and unlike inthe observations, there is no discernible differences ofin SSW frequencyies between QBO westerly (QBO-W) and QBO easterly (QBO-E) phases. The Asia-Pacific subtropical jet (APJ) shifts significantly equatorward during QBO-W compared to QBO-E in observations, butwhile this the APJ shift is not robust across models, regardless of the ENSO phases. In the tropics, the sign and spatial pattern of the QBO precipitation response vary widely across models and experiments, indicating that any potential QBO signal is strongly modulated by the prevailing ENSO phases of ENSO. Overall, the QBOi models exhibitshow unrealistically weak QBO wind amplitudes in the lower stratosphere, which maycould explainexplain the weak polar vortex and APJ responses, as well asand the weak precipitation signals in the tropics. In contrast, tThe QBO teleconnection withto the Walker circulation duringin boreal summer and /autumn shows a consistent signals in bothacross observations and and most models. Specifically, , with the QBO-W phase is characterized byfeaturing upper-level westerly and lower-level easterly anomalies over the Indian Ocean–Maritime Continent relative to the QBO-E phase, although theits amplitude and timing of these anomalies remainare model-dependent. Notably, theThis influenceimpact of the QBO phase on the Walker circulation appears not to be insensitive to the ENSOthe phase of ENSO.

Short summary (500 characters, incl. spaces)

Links between the stratospheric Quasi-Biennial Oscillation (QBO) and atmospheric circulations in the tropics, subtropics, and polar regions, as well asand their modulation by the El Niño–Southern Oscillation, are examined through model experiments. The QBO polar vortex QBO connectionlinks isare reproduced by a multi-model ensemble at aboutwithin a half ofthe observed amplitude. WeakPoor performance of QBO signals in these tropics, subtropics, and polar regions is likely due to unrealistically weak QBO amplitudes in the lower stratosphere.

Key words: stratosphere-troposphere coupling, teleconnection, QBO, ENSO

1 Introduction

The Quasi-Biennial Oscillation (QBO) and the El Niño–Southern Oscillation (ENSO) are the leading modes of climate variability in the tropical stratosphere and tropical troposphere, respectively. The QBO is a semi-periodic wind variation characterized by downward-~~-~~propagating easterly and westerly wind regimes in the equatorial stratosphere, with an average period of ~~about~~approximately 28 months (Baldwin et al., 2001; Anstey et al., 2022b). It represents~~The QBO is~~ an important source of predictability due to its long timescale and ~~its~~ teleconnections extending beyond~~outside~~ the tropical stratosphere. The QBO is primarily driven by vertical momentum fluxes from~~due to~~ upward-propagating equatorial wave activity generated by tropospheric convective systems (Lindzen and Holton, 1968; Holton and Lindzen, 1972; Plumb and McEwan, 1978).

Over the past two~~a couple of~~ decades, atmospheric general circulation models (AGCMs) and Earth system models (ESMs) ~~are~~have ~~being~~increasingly included~~developed to include an~~ internally-~~-~~generated QBOs ~~to represent more realistic modes of internal variability~~ (e.g. Butchart et al., 2018). To simulate a realistic QBO, ~~M~~most of these models require parameterization of unresolved gravity waves ~~to simulate an internally generated QBO~~, ~~including~~ specific treatments~~conditions~~ of parameterized and/or resolved convection, high horizontal and vertical resolution, and weak implicit and explicit grid-scale dissipation (Anstey et al., 2022b). Although the QBO is primarily an equatorial stratospheric phenomenon, it influences~~impacts~~ the climate system beyond~~outside~~ this region through~~via~~ teleconnections. ~~We can obtain a~~A deeper~~more in-depth~~ understanding of QBO teleconnections—including ~~(~~extratropical impacts, tropical and subtropical effects~~impacts~~, and their interactions with other phenomena—~~)~~can be achieved by intercomparing ~~many~~ state-of-the-art, stratosphere-resolving models that simulate ~~a~~ QBO-like oscillations in the tropical stratosphere.

The QBO ~~can~~ influences the Northern Hemisphere (NH) winter stratosphere by modulating planetary-scale waves that affect~~distort~~ the stratospheric polar vortex. The observed statistical relationship between ~~the~~ QBO phase and polar vortex strength is commonly referred to as the ~~Holton-Tan~~Holton–Tan effect (Holton and Tan, 1980, 1982). When the QBO in the lower stratosphere (~50 hPa) is in its westerly phase (QBO-W), the polar vortex tends~~is observed~~ to be stronger and colder, and a reducing~~the~~ likelihood of sudden stratospheric warming (SSW) events ~~is reduced~~. Conversely, during~~when~~ the ~~QBO is in its~~ easterly phase (QBO-E), the stratospheric polar vortex is weaker, warmer, and more disturbed. The ~~underlying~~ mechanisms underlying~~for~~ this effect have been extensively investigated~~examined~~ in both~~by many~~ observational and modeling studies. ~~The mechanism proposed by~~ Holton and Tan (1980) proposed that~~to explain~~ this effect~~relationship~~ results from~~involves~~ a latitudinal shift of the zero-wind line, which acts as an effective waveguide for upward-propagating planetary waves in the NH winter stratosphere (Holton and Tan, 1980; Baldwin et al., 2001; Anstey and Shepherd, 2014; Watson and Gray, 2014; Gray et al., 2018; Lu et al., 2020; Anstey et al., 2022b). A related ~~similar but distinct~~ mechanism suggests that~~involves~~ planetary waves interact~~ing~~ with ~~the~~ zonal wind anomalies associated with the QBO-induced secondary circulation, without~~not~~ requiring ~~zero-wind-line-induced~~ wave breaking induced by the zero-wind-line (Ruzmaikin et al., 2005;

Naoe and Shibata, 2010; Garfinkel et al., 2012b; White et al., 2015; Naoe and Yoshida, 2019; Rao et al., 2020; Anstey et al., 2022b). A tropospheric pathway of the ~~Holton-Tan~~Holton–Tan relationship has also been proposed. In ~~T~~this mechanism, ~~involves~~ Rossby waves propagat~~ing~~e from regions of tropical convection to higher latitudes, including the Aleutian low-pressure region, and disturb the stratospheric polar vortex ~~is disturbed by~~through the subsequent upward wave activity flux into the stratosphere, which is modulated by~~through~~ tropospheric processes (Yamazaki et al., 2020). Although the relative importance of these ~~different~~ mechanisms remain~~s~~ somewhat unclear, ~~due to the QBO's long timescale~~ these teleconnections may enhance~~lead to increased~~ the predictability of the extratropical stratosphere on sub-seasonal time scales due to the QBO's long periodicity (Boer and Hamilton, 2008; Scaife et al., 2014; Garfinkel et al., 2018).

It~~The QBO~~ has also been suggested ~~to~~that the QBO affects the tropical troposphere by modifying deep convective activity and vertical wind shear near~~along~~ the tropopause (Gray et al., 1992; Collimore et al., 2003). The QBO-induced zonal-mean meridional circulation modulates the ~~temperature~~ vertical temperature profile in the equatorial upper troposphere~~–and~~ lower stratosphere (UTLS), producing~~leading to~~ a QBO signature in tropical tropopause temperature and wind. Although the notion~~idea~~ of a "direct effect" of the QBO on the tropical and subtropical UTLS had been discussed in the literature since the 1960s, it was not ~~yet~~ widely accepted until the early 2000s (Hitchman et al., 2021). ~~Recently a~~A possible downward influence of the QBO on the tropical troposphere has also been found in the Madden–Julian Oscillation (MJO) (Yoo and Son, 2016; Marshall et al., 2016; Son et al., 2017; Martin et al., 2021; Elsbury et al., 2025). For more recent reviews of stratosphere–troposphere coupling in the tropics, see Haynes et al. (2021) and Hitchman et al. (2021).

Observational and modeling studies suggest that the interannual variability of tropical precipitation is, at least partially, modulated by the phase of the QBO (Collimore et al., 2003; Liess and Geller, 2012; Gray et al., 2018). In observations, the QBO signal in tropical precipitation shows zonally asymmetric patterns, for example~~e.g.,~~ wetter conditions in the eastern Pacific Intertropical Convergence Zone (ITCZ) during QBO-W compared to QBO-E (Gray et al., 2018;~~,~~ Serva et al., 2022). The similarity between ~~the~~ QBO and ENSO signals in observations may result from~~could potentially be caused by~~ the higher number of El Niño events coinciding with QBO-W than with QBO-E (García-Franco et al., 2022). Serva et al. (2022) analyzed the simulated precipitation in Atmospheric Model Intercomparison Project (AMIP)-type simulations from the first phase of Quasi-Biennial Oscillation initiative (QBOi) experiments (Butchart et al., 2018). ~~and~~They found that those simulations have a limited ability to reproduce the observed modulation of the tropical tropopause-~~—~~level processes, even after removing~~subtracting the~~ variability associated with the ENSO index. In these sea-surface temperature (SST)-forced, free-running simulations, the east Pacific ITCZ precipitation response to the QBO, which resembles the observed pattern, is reproduced~~simulated~~ by many, though not all, models (Fig. 11 of Serva et al. (2022)). However, the simulated QBO signal in~~on~~ the tropopause is generally underestimated or ~~not~~ unrealistic in these models.

In addition~~Also~~, Rao et al. (2020b) explored ~~and evaluated~~ three dynamical pathways~~—~~through the (stratosphere polar vortex, North Pacific via~~through the~~ subtropical downward arching zonal winds, and tropical convection~~pathways)—~~ for QBO impacts ~~of the QBO~~ on the troposphere, using ~~the~~ state-of-the-art CMIP5/6 models with a spontaneously generated QBO. They found that more than half of the models could~~can~~ reproduce at least one of the three pathways,~~,~~ but few models could~~can~~

reproduce all ~~of the~~ three ~~route~~pathways. Using similar SST-forced, as well as coupled ocean–~~-~~atmosphere ~~coupled~~ simulations with a single model, García-Franco et al. (2023) suggested that the simulated precipitation response to the QBO strongly~~is heavily~~ depends~~ent~~ on the state of ENSO and the Walker circulation, the strength of the QBO, and ~~the~~ ocean–~~-~~atmosphere coupling.

In the subtropics, the QBO has a direct influence on~~of the QBO modulates~~ the subtropical jet ~~by~~through its~~the QBO~~ secondary circulation. Observational studies have indicated that the QBO can affect the subtropical jet variability, particularly~~especially~~ in the Pacific sector (e.g. Garfinkel and Hartmann, 2011a; 2011b). During QBO-W, a horseshoe-shaped zonal wind anomaly forms in the UTLS~~upper troposphere and lower stratosphere~~ associated with an~~the~~ equatorward shift of the Asian-Pacific jet (APJ) (Crooks and Gray, 2005; Simpson et al., 2009)~~,~~ This~~and the resultant~~ response is evident~~found~~ even ~~in the East Asian~~ near the surface over East Asian (Park et al., 2022; Park and Son, 2022). A study using a QBO-resolving multi-model ensemble found no clear evidence of a QBO teleconnection to the subtropical Pacific-sector jet (Anstey et al., 2022c), whereas~~while~~ another multi-model study found that seven out of 17 models captured this effect (Rao et al., 2020b).

ENSO teleconnections to the NH winter stratosphere have been widely reported in numerous~~a large number of~~ observational studies (van Loon and Labitzke, 1987; Camp and Tung, 2007; Garfinkel and Hartmann, 2007; Song and Son, 2018) and ~~in~~ modeling studies (Taguchi and Hartmann, 2006; García-Serrano et al., 2017; Palmeiro et al., 2017, 2023; Trascasa-Castro et al., 2019; Weinberger et al., 2019). During El Niño winters, the polar vortex tends to be~~is~~ weaker, and the polar region becomes~~is~~ warmer compared to~~than~~ ENSO~~-~~-neutral winters~~years~~, whereas~~while during~~ strong La Niña winters~~,~~ are associated with a weakening of the Aleutian low and destructive linear interference with the climatological wave pattern ~~was identified~~ (Iza et al., 2016). Observations indicate~~showed~~ that SSW events occur more frequently~~preferentially~~ during both El Niño and La Niña winters than during ENSO-neutral winters (Butler and Polvani, 2011; Garfinkel et al., 2012a). However, ~~there might be~~ sampling errors may arise due to the relatively short observational record (Domeisen et al., 2019), and the reported increase~~d~~ in SSWs during La Niña winters is~~were~~ sensitive to the ~~SSW~~ definition of SSWs used (Song and Son, 2018). The ~~O~~observed relationships between ENSO and SSWs were often not reproduced~~replicated~~ in~~by~~ models. Models typically~~often~~ simulate~~d~~ ENSO events and teleconnections that appear~~were~~ considerably more linear than~~compared to~~ the ~~available~~ observational evidence~~data~~ suggests (Domeisen et al., 2019). For example, simulations with a chemistry-climate model showed~~there is~~ no indication of ~~any~~ nonlinearities between El Niño and La Niña~~EN and LN~~, and~~while~~ SSW frequencies for both phases~~EN and LN~~ were found to be~~are both~~ similar~~, using a chemistry-climate model~~ (Weinberger et al., 2019). Trascasa-Castro et al. (2019) investigated the effect of ~~variations in~~ENSO amplitude variations on European winter climate using~~with~~ idealized SST anomalies and ~~they did not find~~found no evidence of ~~a~~ saturation in~~of~~ the stratospheric pathway under~~due to~~ strong El Niñ~~n~~o forcing~~, as suggested in previous literature~~. Systematic model biases in atmospheric winds and temperatures likely~~would~~ affect the representation of the ENSO–~~-~~SSW teleconnection (Tyrrell et al., 2022).

ENSO exerts~~has~~ significant impacts on ~~the~~ global atmospheric circulation~~s~~, and QBO teleconnections may also be modulated~~influenced~~ by El Niño and La Niña. The QBO itself is affected by ENSO, with weaker QBO amplitude and faster QBO phase propagation under El Niño than under La Niña conditions (Taguchi, 2010a). Previous studies ~~that~~ investigating~~ed~~

the joint effects of QBO and ENSO on winter polar vortex variability in winter have suggested that their interactions are nonlinear, withinsofar as the Holton-TanHolton–Tan relationship is found to bebeing significant duringin the La Niña phase but much weaker duringin the El Niño phase (Wei et al., 2007; Garfinkel and Hartmann, 2008; Calvo et al., 2009; Richter et al., 2011; Hansen et al., 2016). A recent observational study (Kumar et al., 2023) examinedinvestigated the combined effects of the QBO and ENSO inon modulating the extratropical winter troposphere during the 1979–2018 period. They found that during La Niña, QBO signals in the polar vortex were amplified, and the polar vortex and subtropical jet were enhanced under QBO-W. During El Niño, a stronger subtropical jet and athe warmer polar vortex were present under QBO-W. Ma et al. (2023) assessed the synergistic effects of the QBO and ENSO on the North Atlantic winter atmospheric circulation using model output and reanalysis data, and foundshowing that the QBO and ENSO have theira nonlinear combined effect on North Atlantic surface pressure anomalies, which arises frombecause different pathways depending onare preferred for different the QBO and ENSO combinations of QBO and ENSO. In contrast, Walsh et al. (2022) demonstrated that the polar vortex weakens more strongly when El Niño coincides withand QBO-E easterly occur together than would be expected fromby the sum of their individual effects (Walsh et al., 2022). However, there remains no cleara lack of consensus on the nature of nonlinearity in QBO–ENSO teleconnections withinin the extratropical circulation of the NH winter stratosphere.

In the tropical troposphere, the QBO and ENSO teleconnections remain less understood than those in the extratropics. Only Aa limitedrelatively small number of studies have analyzed tropical tropospheric QBO teleconnections using models capable ofthat simulateing the QBO (Rao et al., 2020; García-Franco et al., 2022, 2023; Serva et al., 2022). As noted by García-Franco et al. (2022, 2023), the observational record is likely too short to separate QBO teleconnections in the tropical troposphere from the strong influence of ENSO, sincebecause El Niño winters often coincide with the westerly phase of the QBO.

The goal of thispresent study isaims to reexamine QBO teleconnections to both the extratropics and tropics andbut now address combined QBO–ENSO influences using a new dataset of idealized ENSO experiments. Model experiments, thatwhich can are capable ofseparateing the influences of QBO and ENSO influences on the extratropical and tropical troposphere outside of the QBO region, are a valuable tools tofor investigatingstudy the modulation of QBO teleconnections by ENSO. To isolate the QBO teleconnections from theENSO influences of ENSO, we conduct model integrations with annually -repeating prescribed SSTs representativecharacteristic of typical El Niño and La Niña conditions, thereby removing ENSO diversity from consideration.

The Quasi-Biennial Oscillation initiative (QBOi), an international project supported by the World Climate Research Programme (WCRP) core project Atmospheric Processes And their Role in Climate (APARC), has focused on assessing internally generated QBOs in climate models and improving model simulation ofunderstanding of how to simulate a realistic QBO (Butchart et al., 2018; Anstey et al., 2022a,c; Bushell et al., 2022; Richter et al., 2022). In order tTo investigatestudy QBO and ENSO teleconnections and their mutual interactions, QBOi has coordinated additional experiments building on the QBOi phase-1 experiments, referred to here as the “QBOiENSO” experiments,. These experiments employusing participating QBOi atmospheric general circulation models (AGCMs) and Earth System Models (ESMs) forced by prescribed "perpetual El Niño" and "perpetual La Niña" SSTs (Kawatani et al., 2025).

In this paper, we have examined QBO teleconnections modulated by ENSO and evaluate their robustness using a~~this~~ multi-model ensemble of QBO-resolving models that have run the QBOiENSO experiments~~,~~ We compare these results~~and evaluated them by comparison~~ with those from~~against~~ the QBOi phase-1 "Experiment 2", which represents the control case of ENSO-neutral conditions. Further details of ~~how~~ the QBOiENSO experiment~~s~~al design are ~~constructed can be~~ provided~~found~~ in Kawatani et al. (2025). The structure of this~~the~~ paper is as follows:~~.~~ Section 2 describes the datasets of the QBOiENSO experiments and observations, along with~~and~~ the analytical~~sis~~ methods employed. Section 3 characterizes the combined effects of QBO–ENSO teleconnections on the polar winter stratosphere (~~Holton-Tan~~Holton–Tan relationship). Sections 4 and 5 present the subtropical and tropical impacts of the QBO modified by ENSO, respectively. Finally, Section 6 provides more discussion and a summary of our findings~~ and discussion~~.

2 Data and Methods

We use nine AGCMs and ESMs participating in the QBOi project~~,~~ and conduct~~ing~~ three experiments. The first one is the QBOi Experiment 2 using a climatological annual cycle of SST and sea ice conditions (Butchart et al., 2018). We hereafter refer to it as the control (CTL) experiment. The other two experiments are the QBOiENSO experiments, QBOiElNino and QBOiLaNina (Kawatani et al., 2025). They are ~~also~~ time-slice experiments consistent with the QBOi Experiment 2 design~~,~~ but with prescribed "perpetual El Niño" and "perpetual La Niña" SST anomalies~~ are used here~~. They are referred to hereafter as the EN and LN experiments, respectively. The models that performed the CTL, EN, and LN experiments are EC-EARTH3.3 (hereafter EC-EARTH for short), ECHAM5sh, EMAC, GISS-E2-2G (GISS~~ for short~~), LMDz6 (LMDz~~ for short~~), MIROC-AGCM-LL (MIROC-AGCM~~ for short~~), MIROC-ESM, MRI-ESM2.0, and CESM1(WACCM5-110L) (WACCM for short). Their characteristics have been described in Butchart et al. (2018) and Kawatani et al. (2025). MRI-ESM2.0 (Yukimoto et al., 2019) is an updated version of the model documented in Butchart et al. (2018), and it includes changes aimed at improving the mode~~l~~led QBO (Naoe and Yoshida, 2019). The lengths of ~~M~~model integrations~~ years~~ for each of the three experiments are presented in Table 1. Due to data availability issues, EMAC is not included in the results in Sections 4 and 5.1 below.

Table 1. The length of the ~~M~~model integrations~~ years~~

Model name	Years	
	[1]QBOi Exp2	[2]QBOi ENSO
[3]EC-EARTH	101-yr	101-yr
[4]ECHAM5sh	50-yr	40-yr
EMAC	106-yr	106-yr
GISS-E2-2G	3 × 30-yr	3 × 30-yr
LMDz	70-yr	82-yr

MIROC-AGCM	3 × 30-yr	100-yr
MIROC-ESM	3 × 100-yr	100-yr
MRI-ESM2.0	30-yr	50-yr
[5]WACCM	3 x 30-yr	100-yr

[1]QBOi Experiment 2 (or CTL experiment)

[2]QBOi ENSO experiments (QBOiElNino and QBOiLaNina experiments)

[3]EC-EARTH3.1 for QBOi Exp2 and EC-EARTH3.3 for QBOi ENSO

[4]Only the realization labelled r2i1p1 is used in ECHAM5sh.

[5]CESM1 (WACCM5-110L) is abbreviated to WACCM.

Observed teleconnections are quantified using a modern reanalysis dataset, the European Centre for Medium-Range Weather Forecasts (ECMWF) fifth generation atmospheric reanalysis (ERA5; Hersbach et al., 2020) overin 1959–2021. The representation of the QBO in ERA5 as compared to other reanalyses is evaluated by Pahlavan et al. (2021) and Naoe et al. (2025). Observed precipitation is evaluated using the dataset of the Global Precipitation Climatology Project (GPCP; Adler et al., 2003, 2016) dataset overin 1979–2022. Because theThe design of QBOiENSO experiments used the Japan Meteorological Agency's (JMA) defined NINO.3 index (https://ds.data.jma.go.jp/tcc/tcc/products/elnino/index/index.html), and so the classification of ENSO phases is based on this index. We note that the QBOiENSO experiments are idealized;, therefore, we mostly rely on observation-based datasets to determine whether the model responses are at least qualitatively in agreement with the (short) observational record.

To determine if observed teleconnections are well representedmanifested in the model runs, the models and observations are compared by applying the same QBO phase definitions to the models that are optimal for the observed teleconnections. Here, we use 'standard' indices (e.g., 50-hPa equatorial wind for the QBO), without adjusting them on a model-by-model basis, for all analyses presented in Sections 3, 4 and 5.1. This can facilitates comparison with other works. As noted by Anstey et al. (2022c), different QBO indices can maximize the response of different teleconnections (e.g. Gray et al., 2018). Thus, making these choices can account for the diversity of QBO signals (tropical convection, Walker circulation, subtropical jet response, extratropical basic-state zonal-mean flow for the Holton-TanHolton–Tan effect, etc.), which may lead to variations in the diagnosed QBO teleconnections. Zonal wind biases need to be carefully considered when defining the QBO phases in model outputs, as noted by Serva et al. (2022). Here, QBO phases are identified when the deseasonalized westerly and easterly zonal-mean zonal wind (QBO-W and QBO-E) averaged over 5° S–5° N (weighted by cosine of latitude) exceeds a given threshold value at selected pressure levels. Specifically, QBO-W and QBO-E are classified from the December-January-February (DJF) zonal wind at 50 hPa using > 0.5 σ (standard deviation) and < −0.5 σ in Section 3.1 (Figs. 2 and 3), using ≥ 0 m s^{-1} and < 0 m s^{-1} in Section 3.2 (Fig. 5), using ≥ 2 m s^{-1} and ≤ −2 m s^{-1} in Section 5.1 (Figs. 8, 9, and 10), and from the February-March zonal wind at 70 hPa using > 0.5 σ and < −0.5 σ in Section 4 (Figs. 6 and 7). In Section 5.2, the strongest signal in each model is identified, considering model diversity and biases in the simulated QBOs and tropical convection, from May to November with QBO definitions provided in the legend of Figs. 11 and 12; the analysis is summarized in Fig. 13. This approach is used to highlight the model dependency and seasonality of the QBO signal on the Walker circulation. Using a common definition for QBO phases in terms of the pressure level and season provides similar but weaker results (see Figs. S9, S10 and S11 using the summer zonal wind at 70 hPa).

The ENSO composites in observations are obtaineddone in the extratropics and subtropics for individual seasons in (Sections 3, 4, and 5.2), whileand in the tropics for individual months in (Section 5.1). In Section 5.2, the Bonferroni correction, as described by Holm (1979), is used for the two-sided *t*-test when the QBO phase is not defined using the preferred 70 hPa level during June-July-August (JJA). In this method, the significance level of the statistical test is adjusted by dividing it by m, the number of tests performed, becoming more restrictive by increasing the confidence level. For instance, if the QBO definition is modified by season only, $m = 2$; if it is modified by both season and vertical level, $m = 3$. Accordingly, $\alpha' = \alpha/m$, where $\alpha = 0.025$ (the 5% significance level for a two-sided test), and α' denotes the adjusted threshold; implying that the corresponding p-value musthas to be smaller to reject the null hypothesis.

3 QBO teleconnections: the extratropical ~~route~~pathway

This section investigates the extratropical pathway of the QBO teleconnection modulated by ENSO, with a focus on the Holton–Tan effect and SSW statistics. A previous study on~~about~~ QBO teleconnections ~~of the QBO in~~using a multi-model ensemble of QBO-resolving models (Anstey et al., 2022c) found that QBOi models underestimated the polar vortex response to the equatorial zonal wind at 50 hPa compared with~~in comparison to~~ reanalyses. They suggested that these~~such~~ weak responses were likely due to model biases~~errors~~, such as systematically weak QBO amplitudes near 50 hPa, which affected~~ing~~ the QBO teleconnection. Since~~Because~~ most of the models used here for~~that have run~~ the ~~QBOiElNino (~~EN~~)~~ and ~~QBOiLaNina (~~LN~~)~~ experiments ~~considered here~~ are the same as those~~models whose QBOiExp2 (CTL) runs were~~ analyzed by Anstey et al. (2022c) in their CTL experiments, the EN and LN ~~runs~~experiments may similarly underestimate the polar vortex response to the QBO. ~~This section investigates the extratropical route of the QBO teleconnection modulated by ENSO. First, we examine the Holton-Tan effect, and then show the SSW statistics.~~

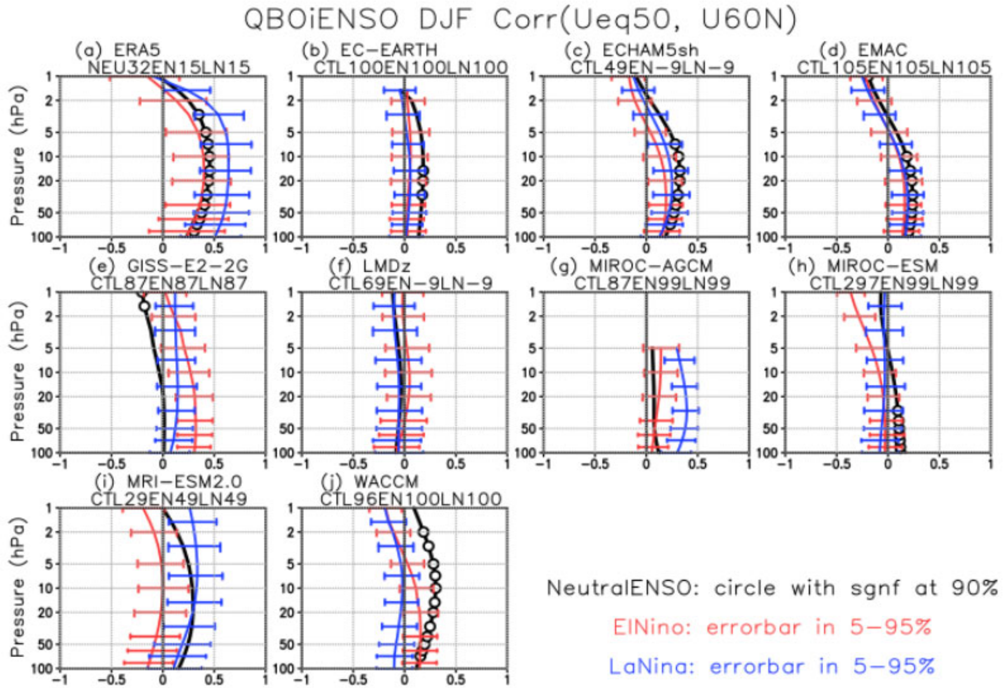

3.1 ~~Holton-Tan~~Holton–Tan relationship

Figure 1: Vertical profiles of the correlation coefficient between the QBO zonal wind at 50 hPa, averaged over 5° S–5° N, and the polar -vortex zonal wind at 55°–65° N duringin December-January-February (DJF) in CTL (black), EN (red), and LN (blue) experimentsfor QBOi models, as well as forand ENSO-neutral (black), El Niño (red), and La Niña (blue) winters in ERA5. Circles denoterepresent statistical significance at the 90 % level for the CTL/ENSO-neutral,. and Red and bluehorizontal bars indicaterepresent the 5–95 % confidence intervalranges, using a bootstrap method repeating 1000 times forin EN / El Niño and LN /experiments for the models as well as El Niño and La Niña winters for ERA5, calculated using a bootstrap method with 1000 times repetition. The Nnumber of winters available for each model run andfor each experiment (ENSO phase) is shown inare displayed at the upper panel. For example, "NEU32EN15LN15"' in the ERA5 panel indicatesmeans there are 32 ENSO-neutral, 15 El Niño, and 15 La Niña winters, respectively.

Figure 1 shows the DJF correlation coefficient in DJF between the 50 hPa equatorial zonal wind at 5° S–5° N and the polar vortex strength at different altitudes in the CTL, EN, and LN experiments, together with ENSO-neutral, El Niño, and La Niña winters fromfor the ERA5 reanalysis. In ERA5the reanalysis, correlations are maximized over a fairly deep layer ofin the polar vortex, reachpeaking 0.63 at 15 hPa during La Niña and 0.40 during El Niño. The correlation during the ENSO-neutral winters is slightly stronger than that duringof El Niño winters. The uncertainty range (horizontal bars) representsshows the 5–95% confidence intervalsrange of correlation coefficients derived from bootstrap resampling. Although For La Niña, the confidence intervals for La Niña clearly excludess zero in the stratosphere, whereas for El Niño theythe confidence for El Niño areis close to zero at many altitudes, indicating substantialdemonstrating large uncertainty in the strength of the correlation especially duringfor El Niño and ENSO-neutral winters.

Most of the model correlations exhibitshow smaller uncertaintiesy than ERA5 due to having larger sample sizes. Models such as (ECHAM5sh, EMAC, EC-EARTH, MIROC-ESM, MRI-ESM2.0, and WACCM) displayhave positive correlation profiles in CTLENSO-neutral, although these correlations arealbeit weaker than incompared to ERA5reanalysis. Most models do not show a significant correlations in EN;, and only four models (MRI-ESM2.0, ECHAM5sh, EMAC, and MIROC-AGCM) out of nine9 reproduce observed positive correlations with confidence intervals excluding zero at certainsome altitudes. It is noted in Fig. 2 of Kawatani et al. (2025, their Fig. 2) presentedfrom their simple, time -–height cross-sections of the monthly and zonal-mean equatorial zonal winds over the equator in the EN and LN simulations, showing that the QBO in the ECHAM5sh infor the EN experimentwasis irregular, with stalling in the downward propagationphases of both easterlies and westerlies. They also showed that the QBOs in GISS and LMDz infor the LN experiment wereare more irregular, withand westerly phases sometimes failing to propagate into the lower stratosphere. These results indicate that most models exhibitshow weak positive correlations consistent inwith the same sign withas ERA5the reanalysis, but in most cases these correlations are not statistically significant. This suggestsmeans that inter-model differences in the QBO–-polar vortex relationship, or differences between experiments withinfor the same model, may not be clearly distinguishable.

Figure 2 presentsshows composite differences inof the zonal-mean zonal wind between QBO-W and QBO-E phases acrossin the CTL, EN, and LN experiments. ERA5 clearly capturesrepresents the Holton-TanHolton–Tan relationship under all three ENSO conditions (neutral, El Niño, and La Niña). The QBO teleconnection to the NH winter stratospheric polar vortex is most strongly correlatedthe strongest in correlation with the QBO amplitude of the QBO at 50 hPa (Anstey et al., 2022c). The difference in vortex strength difference in DJF between QBO-W and QBO-E peaks at approximatelyroughly 10 m s^{-1} in the middle mid-stratosphere (near 10 hPa) during DJF duringfor the ENSO-nNeutral and El Niño wintersgroups, with the strongestand the response occurringis strongest duringin La Niña winters, reachingwith a peak value of 15 m s^{-1}. No model reproduces the observed -strength of the Holton-TanHolton–Tan relationship acrossin all three experiments (CTL, EN, and LN). Only two of the models (MRI-ESM2.0 and WACCM) exhibitreproduce observed responses within a half of the observed amplitude in CTLfor the ENSO-neutral case (MRI-ESM2.0 and WACCM).; Furthermore,and only the MRI-ESM2.0 exhibitsalso shows a stronger QBO impact on the QBO on the vortex inunder the LN condition than undercompared with EN condition, although(however, thisthat model produces an incorrecthas the wrong sign response infor EN). In LN, four models (ECHAM5sh, GISS, MIROC-AGCM, and MRI-ESM2.0) are better at reproducceing the observed response, peaking at a modestslight amplitude of ~3 m s^{-1} in the polar vortex region. GISS shows a significant difference in EN, and a significant LN response in LN just equatorward of 60° N.

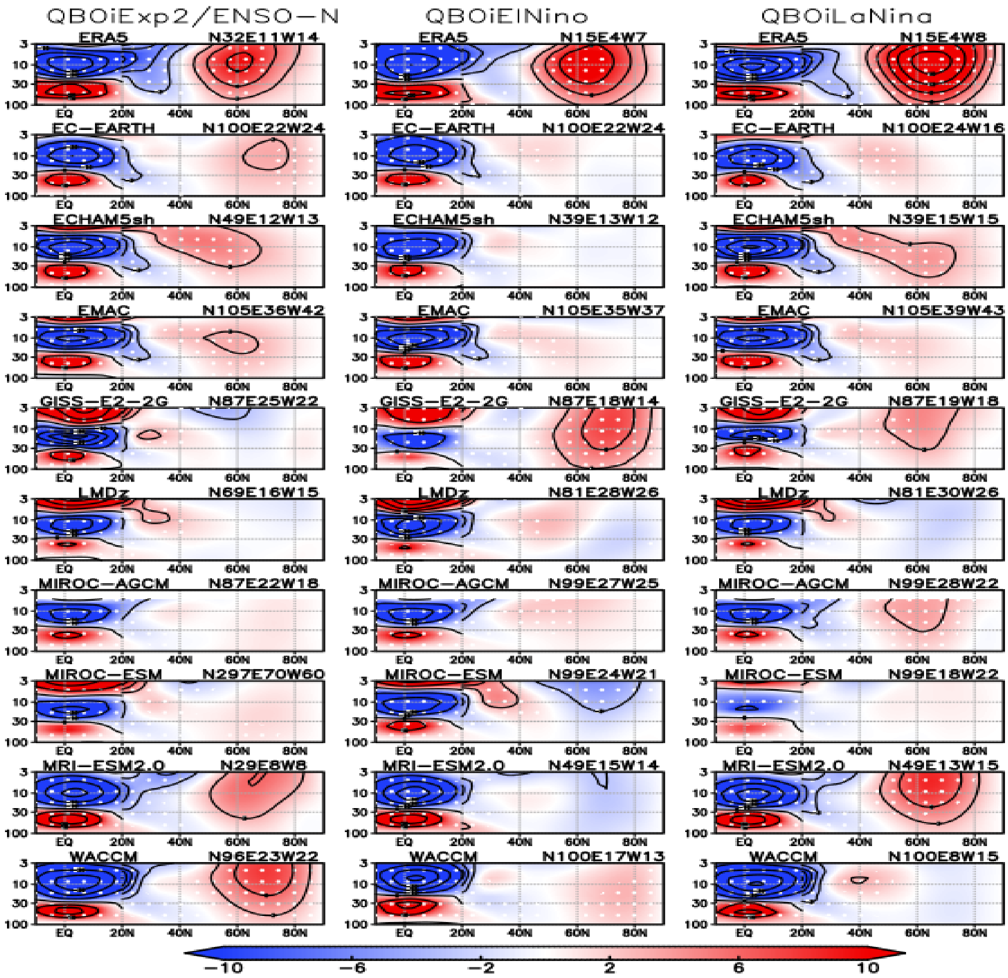

Figure 2: Composite differences in~~of~~ the DJF ~~-~~mean zonal-mean zonal wind between the QBO-W and QBO-E phases, shown in the pressure (in hPa)~~– and~~ latitude domain, for~~in~~ the CTL, EN, and LN experiments, as well as for~~including the~~ ENSO~~-~~neutral, El Niño, and La Niña winters based on~~for~~ ERA5. QBO phases are classified using deseasonalized DJF zonal-mean zonal wind at 50 hPa, averaged over 5° S–5° N, with values greater than~~using >~~ 0.5 σ indicating~~for~~ QBO-W and less than~~<~~ −0.5 σ indicating~~for~~ QBO-E. Contour intervals are 3~~(10)~~ m s^{-1} north ~~(south)~~ of 20° N and 10 m s^{-1} south of 20° N. Dots indicate~~represent~~ statistical significance at the 90 % confidence level. The ~~N~~number of winters ~~available~~ for each model run, along with the counts~~and numbers~~ of QBO-E and QBO-W winter~~s classification~~, is shown~~are displayed~~ in~~at~~ the upper~~-~~right corner of each panel. For example, "~~'~~N100E30W41"~~'~~ for CTL in EC-EARTH~~and QBOiExp2~~ indicates~~means there are~~ a total of 100 winters~~in which~~, with 30 winters classified as QBO-E ~~winters~~ and 41 as QBO-W~~winters are classified~~.

One may ask whetherif a model-specific equatorial wind level, such as 30 hPa (e.g., Rao et al., 2020a), isean be more effectiveefficient for models to reproduceing the QBO's impact on the polar vortex (the Holton-TanHolton–Tan effect). We have examined thea relationship of composite differences of zonal-mean zonal wind inbetween polar vortex responses at 60° N and 10 hPa againstand QBO definition at 50 hPa (QBO50) and at 30 hPa (QBO30) (Fig. S1). Most models underestimate the equatorial QBO composite differences at 50 hPa compared withto those at 30 hPa;, and for some models, the QBO is difficult to detect at 50 hPa.; tThese results are similar to those reported bydescribed in Rao et al. (2020a), which was on for CMIP models. However, both panels (QBO50 and QBO30) show that most models underestimate equatorial QBOs amplitude and they are struggleing to reproduce the observed polar vortex responses to the QBO. We also have examined whether model performance inof QBO amplitude and/or climatological polar night jet strength relatesis related to athe model's ability of model to capture the QBO-induced polar vortex responses (not shown), here hypothesizing that the Holton–TanHTR relationship — (the polar vortex) routepathway of the QBO teleconnection — maycould be influencedmanifested by these two factors. QBO amplitudes at 50 hPa are poorly represented infor most models are poor performance, consistentin agreement with previous studies (Bushell et al., 2022; Anstey et al., 2022), while climatological polar vortices duringin NH winter areean be reproduced with the observed strength. These results are consistent with previous QBOi multi-model ensemble studies, whichthat argued that unrealistically weak low-level QBO amplitudes can weaken the QBO teleconnections to the polar vortex

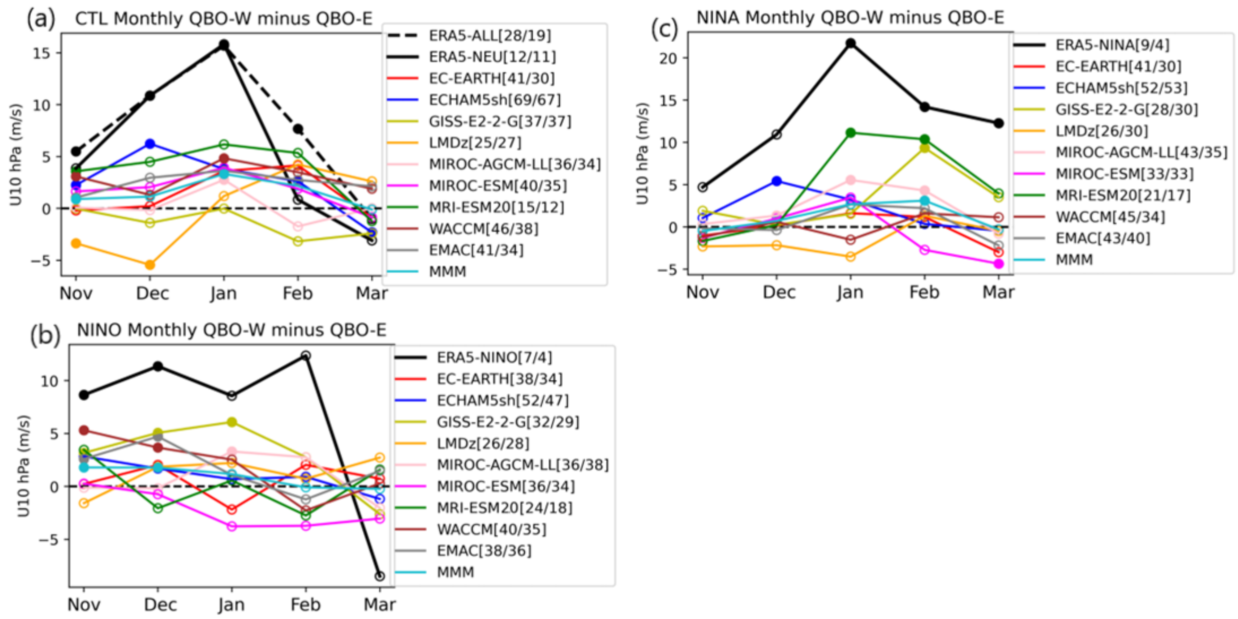

(Richter et al., 2022; Anstey et al., 2022c). In summaryshort, across allfor any of the three experiments, the models generallymore often than not show a stronger polar vortex during NH winter when the 50-hPa QBO wind is westerly, and a weaker vortex when it is easterly, consistent with, but weaker than, the observed response.

Figure 3: (a) Monthly differences (QBO-W minus QBO-E) inof the zonal-mean zonal wind at 10 hPa, averaged over 55°–65° N, as a measure of the stratospheric polar vortex strength for the CTL experiment, along with ENSO-neutral winters in ERA5. QBO phases are classified same as in Fig. 2. Solid dots indicateshow statistically significant differences between the QBO-W and QBO-E phases at the 90 % confidence level, based onusing a Monte Carlo test. The Nnumbers in the legend represent the number ofare the cases included in each QBO phase. The dashed line in panel (a) shows the QBO composite difference in ERA5 when all years (1959–2022) are included in the analysis. MMM denotesmeans thea multi-model mean. (b) Same as (a), but for the EN experiment, along withincluding El Niño winters infor ERA5. (c) Same as (a) but for the LN experiment, along withincluding La Niña winters infor ERA5. The Nnumbers of QBO phase categories (QBO-W, QBO-E) categories forin ERA5 are (12, 11) induring ENSO-Neutral, (7, 4) induring El Niño, and (9, 4) duringin La Niña winters.

The Iintraseasonal Holton–-Tan effects are showninvestigated in Fig. 3, represented bywhich shows the composite difference (QBO-W minus QBO-E) of the monthly zonal-mean zonal wind at 10 hPa, 55°–65° N in the CTL, EN, and LN experiments, together with ERA5. In ERA5, presents thea maximum Holton-TanHolton–Tan effect occurs in January, with a peak of 13 m s^{-1} acrossfor all datathe mean (dashed black line in the top panel)., but tThis difference is reducedlower in February during ENSO-neutral wintersyears (solid black line in Fig. 3a). The Sseasonal evolution of the Holton-TanHolton–Tan effect differsis different between El Niño and La Niña winters; it appearsseems stronger in early and late winters duringfor the El Niño winters (Fig. 3bmiddle panel), and in mid-winter duringfor the La Niña winters (Fig. 3cbottom panel)., However,although it should be notedcautioned that the sample sizes (number of W/E winters) are small for both El Niño and La Niña wintersgroups. Some models (MIROC-ESM and ECHAM5sh) in CTL show a similar seasonal cycle similar to that inas ERA5 for their CTL runs (significant for MIROC-ESM and ECHAM5sh). By contrastAlso, GISS throughoutin all months, as well as LMDz and MIROC-AGCM in certaina few months, in CTL, exhibit a Holton–Tan relationshipan opposite sense to thatthe observed Holton-Tan relationship for CTL. In EN, four models (GISS, WACCM, EMAC, and ECHAM5sh) capture the early -winter response in December, although it is not statistically significant. The Holton-TanHolton–Tan relationship duringin El Niño wintersyears maycould depend on SSW occurrence because of the nonlinear joint effects of QBO and ENSO on the polar vortex, as discussedalready explained in the Introduction. In LN, MRI-ESM2.0 and GISS reproducecapture the observed late-winter response relatively well, whereasand other models do not show noany response or even an opposite response.

3.2 SSW statistics

In this subsection, we examine the QBO impacts on SSW statistics modulated by ENSO and the QBO in the NHnorthern polar region. Previous observational studies have shownindicated that the ratio of SSW frequency between La Niña and ENSO-neutral winters is dependsent on the specific definitiondetails of the SSW definition (Butler and Polvani, 2011; Garfinkel et al., 2012a; Song and Son, 2018), and that SSW statistics are also influenced byhave been shown to depend on model biases (Tyrrell et al., 2022). Figure 4 presentsshows the frequencies of major SSWs,and minor SSWs, and final warming dates in the

NH for ERA5 and the QBOi models. The criteria for~~approach to~~ identifying major SSWs, minor SSWs, and final warming

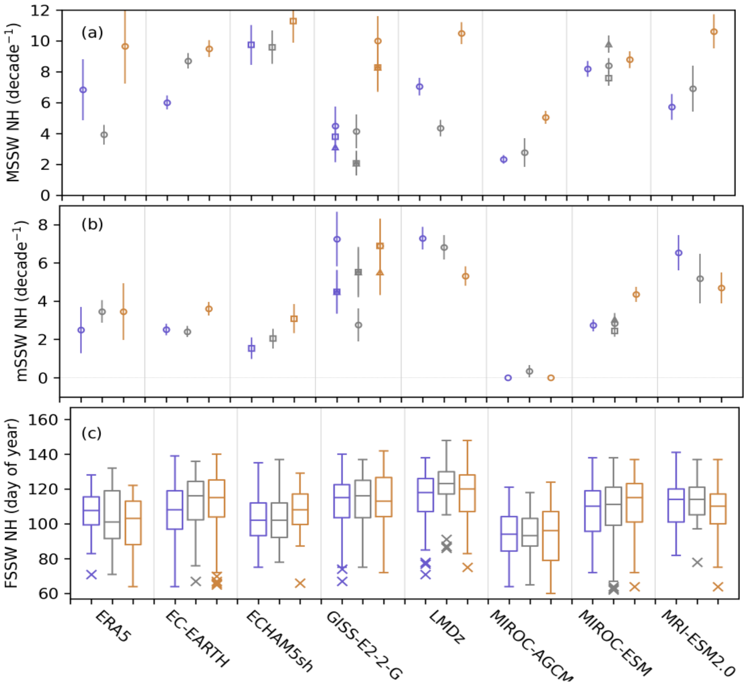

dates follows~~is similar to what was proposed by~~ previous studies (Charlton and Polvani, 2007; Butler et al., 2015). Major SSWs are defined~~identified~~ when the zonal-mean zonal wind at 10 hPa and 60° N (U60)~~westerlies in winter~~ reverse~~are changed~~ from westerlies to easterlies ~~at 60° N and 10 hPa~~ during winter. ~~For m~~Minor SSWs are defined when~~, the zonal wind does not reverse but there is a change in sign of~~ the meridional gradient of the zonal-mean temperature changes the sign without a reversal of U60. A ~~F~~final warming date refers to the seasonal transition from westerl~~y~~ies to easterl~~y~~ies, with winds remaining easterl~~y~~ies thereafter~~for the next months~~.

First, ~~W~~we assess~~consider~~ ~~first~~ the influence of ENSO on SSW frequenc~~y~~ies. In ERA5 (the leftmost triplet in~~of~~ Fig. 4a ~~panel~~), the frequenc~~y~~ies of major SSWs are~~is~~ high ~~in ERA5~~ during both El Niño and La Niña winters~~years,~~ compared to ENSO-neutral winters. Thus, we expect that major SSW frequencies in the QBOi models would resemble~~be similar to~~ the observations, with~~and have~~ fewer events in CTL and more ~~events~~ in EN and LN~~experiments~~. LMDz and GISS reproduce the observed nonlinear ~~observed~~ ENSO response to some extent (Fig. 4a). However, most models simulate~~show~~ more SSWs in~~during~~ EN but~~and they~~ fail to~~do not~~ capture the ~~LN~~ response in LN (e.g., EC-EARTH, MIROC-AGCM, and MRI-ESM2.0). Only one model (ECHAM5sh) reproduces~~shows~~ the observed relationship between the frequency of minor SSWs~~warmings~~ and the ENSO phase~~of ENSO~~, showing~~and it has~~ similar frequencies in CTL and LN, and more events in EN.

Figure 4: SSW statistics — namely, the frequencies of (a) major SSWs, (b) minor SSWs, and (c) final SSW dates — in the Northern Hemisphere~~NH~~ for~~in~~ the CTL, EN, and LN experiments in~~for~~ the QBOi models, along with~~including~~ ENSO~~-~~-neutral, El Niño, and La Niña winters~~years~~ in~~for~~ ERA5, based on their daily data. The order of triplets from left to right is~~are~~ LN / La Niñ~~n~~a (~~LN,~~ purple), CTL / ENSO~~-~~-neutral ~~winter experiment~~ (~~CTL,~~ grey), and EN / El Niñ~~n~~o (~~EN,~~ brown). The ~~F~~frequency (number of events per decade) of ~~(a)~~ major SSWs is defined as the number of ~~(~~reversals of the zonal-mean zonal wind at 10 hPa and 60° N~~;~~ (U60), while~~and~~ the frequency of ~~(b)~~ minor SSWs is defined as the number of ~~(~~reversals of 90°–60° N temperature gradient at 10 hPa without a U60 reversal,~~;)~~ occurring across full seasons. ~~It is noted that multiple marker signs in the same experiment for a model indicate ensemble members (depending on data availability). Uncertainties are estimated at the 5–95% level based on bootstrapping of 10 years of winter months. (c) Boxplots of~~ The final SSW date (day of year)~~,~~ is determined for~~considering~~ full seasons, which is defined as a~~i.e.,~~ period from the ~~westerlies~~ onset of westerlies to the transition~~their turn~~ to easterl~~y~~ies ~~for ERA5 and QBOi models based on their daily data~~. Uncertainties are estimated at the 5–95% confidence level using bootstrapping of 10 years of winter months. Multiple markers within the same experiment of a model indicate ensemble members, depending on data availability.

The final warming date is defined as ~~when~~the transition from winter westerlies to summer easterlies ~~occurs~~ in the polar stratosphere (Butler et al., 2015). If the polar stratosphere is warmer ~~in the polar regions~~, the ~~transition of~~ zonal wind transition to easterlies occurs earlier, whereas~~and~~ if it is colder, the transition is delayed. Hence, we assume that ~~in~~during El Niño/ ~~(~~La Niña~~)~~ winters~~years~~, when the polar stratosphere tends to~~would~~ be warmer/ ~~(~~colder~~)~~ as described in the Introduction, the final warming date may~~might~~ occur~~happen~~ earlier/ ~~(~~later~~)~~. Consistent with this expectation, in ERA5 during La Niña winters (the leftmost triplet of Fig. 4c), the final warming date is ~~more~~ delayed compared with~~than that in~~ ENSO-neutral and El Niño winters~~years~~. GISS and MRI-ESM2.0 also show~~exhibit~~ later final warming dates in LN compared with~~than in~~ EN, consistent with~~which is similar to~~ the observed response (Fig. 4c). In contrast~~On the other hand~~, five models (EC-EARTH, ECHAM5sh, LMDZ, MIROC-AGCM, and MIROC-ESM) fail to~~do not~~ show earlier final warming dates in EN, ~~which is the~~ opposite to the observed response. These results show~~imply~~ that the QBOi models have significant biases in reproducing observed SSW~~s~~ statistics. Large inter-model variability is also evident~~diagnosed~~ in~~by means of~~ the Northern Annular Mode (NAM) index (Eyring et al., 2020) composit~~ed~~ing at 500 hPa, as shown in Fig. S2, where the geopotential heights during LN tend to be lower and ~~there are changes in~~ the intensity of the extratropical signature differs between LN and EN. Inter-model variability in the large-scale response to ENSO may also explain the spread in SSW~~the~~ occurrence ~~of SSWs~~ (e.g.~~i.e.~~, in the GISS and MIROC-ESM models in Fig. 4) due to differences in ~~the~~ simulated tropospheric forcing.

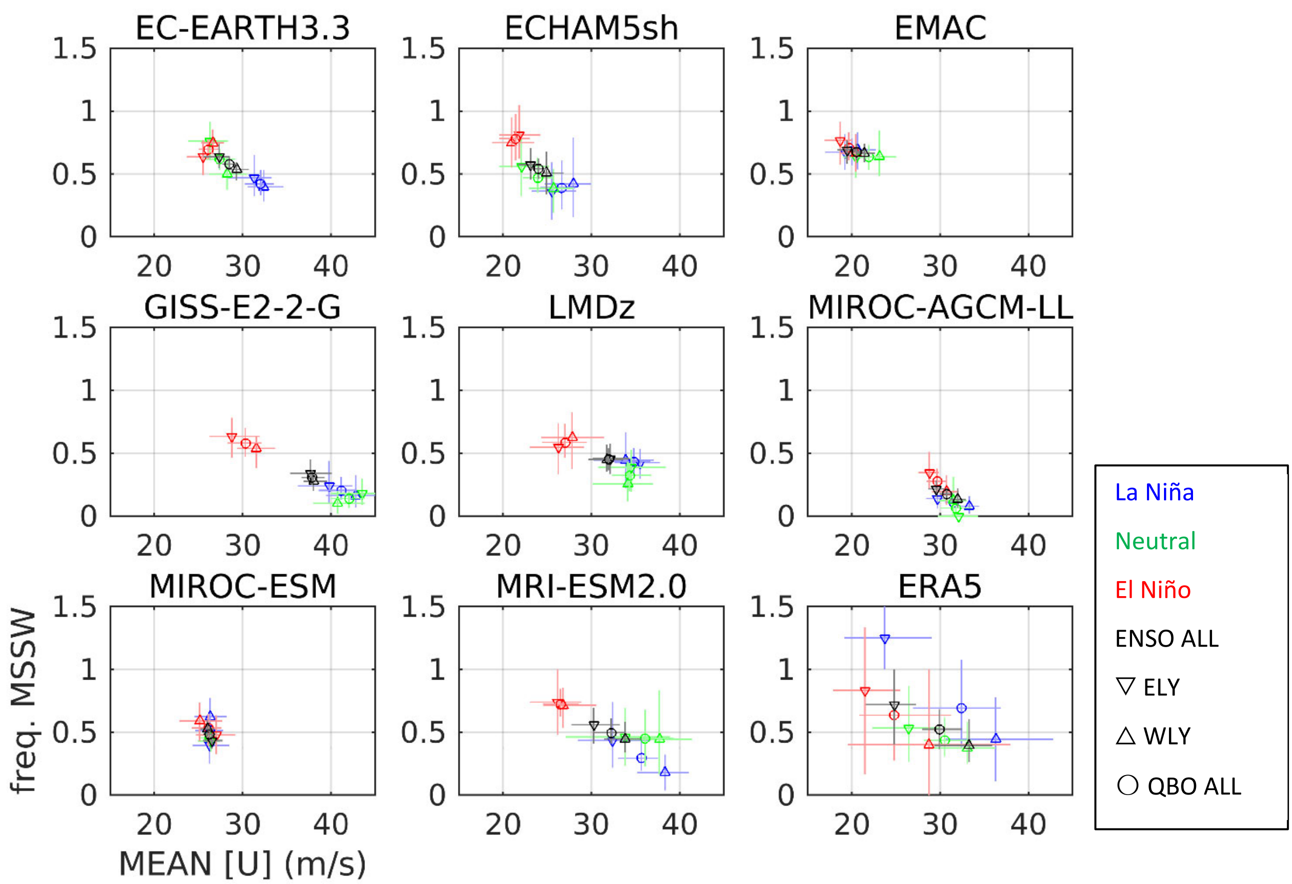

Figure 5: Scatter plots of~~between~~ the winter-mean vortex strength at ~~(~~60° N~~,~~ and 10 hPa~~)~~ versus~~and~~ the major SSW frequency during DJF under~~for~~ different QBO and ENSO conditions. Major SSWs are defined~~identified~~ as ~~a~~ reversals of the daily zonal-mean zonal wind at 60°N and 10 hPa. QBO phases are classified using DJF-mean zonal-mean zonal wind anomalies at 50 hPa, averaged over 5° S–5° N, with anomalies~~using~~ ≥ 0 m s^{-1} indicating~~for~~ QBO-W marked by up-pointing triangles (WLY in panel) and < 0 m s^{-1} indicating~~for~~ QBO-E marked by down-pointing triangles (ELY in panel). The sum of QBO-W and QBO-E is marked by circles (QBO ALL in panel). ~~The A~~anomalies are calculated for each ensemble member of each experiment in~~for~~ the simulation data; for ERA5, they~~those ones are~~ are calculated using all winters~~years~~ from ~~(~~1959 to ~~-~~2021~~ seasons) for the ERA5 data~~. ~~For ERA5,~~ El Niño and La Niña winters in observations are identified when all three DJF months have the El Niño and La Niña classification~~flag, respectively~~. The ~~N~~numbers of QBO phase categories (QBO-W, QBO-E) ~~categories for~~in ERA5 are (24, 15) during~~in~~ ENSO-~~N~~neutral, (5, 6) during~~in~~ El Niño, and (9, 4) during~~in~~ La Niña winters. For each condition~~,~~ and~~each~~ model, the data are randomly resampled 100 times with replacement, and ~~then~~ 95% confidence intervals~~ranges~~ are calculated~~obtained and plotted~~.

Next, we examine~~investigate~~ the influence of the QBO on major SSW frequencies modulated by ENSO during~~in the~~ NH winter. Figure 5 shows scatter plots of~~between~~ the climatological zonal-mean zonal wind at 60° N and 10 hPa against~~and~~ the ~~mean~~ frequency of major SSWs during~~in~~ DJF under~~during~~ two QBO~~-W and QBO-E years~~ phases and~~for~~ three ENSO conditions. In ERA5, major SSW frequencies under QBO and ENSO conditions are clearly ~~likely to be~~ distinguishable.

Averaged over all QBO conditions, the NH polar vortex is stronger duringin La Niña than during El Niño winters, while SSW frequencies are slightly higher duringin La Niña than during El Niño winters, and both are higher than during ENSO-neutral winters. Major SSW frequencies duringin La Niña winters are significantly higher under QBO-E and lower under QBO-W, whereas those duringin El Niño winters, they are indistinguishable between QBO-W and QBO-E. Most QBOi models exhibitare characterized by linear relationshipsdistributions between SSW frequencies and the polar vortex strength. They generally simulateThe EN experiment displays higher SSW frequencies of SSWs in EN than inthe LN experiment, with and SSW frequencies between QBO-W and QBO-E arelittle distinctionindistinguishable between QBO-W and QBO-E. This indicatesshows that polar vortex responses to ENSO conditions in the QBOi models are stronger than their responses to the QBOs phasesin these models. Some models (EMAC, MIROC-AGCM, and MIROC-ESM) have very weak responses to both QBO and ENSO and QBOconditions.

4 The subtropical jet routepathway of QBO teleconnections

This section examines the subtropical jet routepathway of the QBO teleconnection modulated by ENSO, focusing on the APJin the QBOi ENSO experiments. Only the late winter period of (February– to March) is considered, when the subtropical routepathway is strongest in the observations (Garfinkel and Hartmann, 2011a; Park et al., 2022), is considered. Since theThe subtropical jet change in response to the QBO is most pronounced infor the APJ, and so analyses are performed for the zonal wind averaged over the Pacific sector (150° E–150° W). The sensitivity of the QBO–-APJ connection to the ENSO phase is also examined.

The QBO-W minus QBO-E (W–E) composite differences are shown in Fig. 6 for the ENSO-neutral, El Niño, and La Niña winters,, usingfor both ERA5 and QBOi ENSO experiments. In ERA5During the ENSO-neutral winter, thea QBO--W minus QBO-–E anomaly exhibits a distinct horseshoe-shaped pattern extending from the tropical lower stratosphere to the subtropical lower troposphere during ENSO-neutral winters (top-left panel in Fig. 6). This anomalyIt is accompanied by a quasi-barotropic, easterly anomaly in the extratropics. More importantly, the zonal wind anomalies switch sign across the climatological APJ (contour),. This indicatinges that the APJ shifts equatorward during the QBO-W winters compared withto the QBO-E winters. Most models underestimate or fail to reproduce the observed QBO–-APJ connection. The dipolar wind anomalies are much weaker in five models (EC-EARTH, ECHAM5sh, GISS, LMDz, and MIROC-ESM) than those in observations in five models (i.e., EC-EARTH, ECHAM5sh, GISS, LMDz, and MIROC-ESM). Although one lobe of the dipolar wind anomalies is significant in ECHAM5sh and GISS, other models (i.e., EC-EARTH, LMDz, and MIROC-ESM) exhibithave statistically insignificant dipolar wind anomalies. MIROC-AGCM and MRI-ESM2.0 even produceexhibit anomalies of the opposite sign. Such a large inter-model spread is consistent with a previous workstudy (Anstey et al., 2022c). In ERA5, Tthe QBO–-APJ connection differs between El Niño and La Niña winters (top-middle and top-right panels in Fig. 6; Garfinkel and Hartmann, 2010). As the APJ strengthens over the Pacific sector (150° E–150° W) in response to El Niño (compare climatological jet contours; Rasmusson and Wallace, 1983; Mo et al., 1998; Lu et al., 2008), the QBO--induced subtropical wind anomalies intensify~~become stronger~~ near the APJ core~~center~~ during El Niño winters (top-middle panel; Ma et al., 2023). In contrast, the QBO-W minus QBO-E~~W−E~~ anomalies switch sign across the climatological APJ during La Niña winters (top-right panel), when~~as~~ the APJ becomes slightly weaker (compare ~~line~~ climatological jet contours in the top-left and top-right panels). The APJ's response to ENSO is consistently reproduced across models, whereas the ENSO modulation of the QBO~~–~~–APJ connection exhibits~~shows~~ a large inter-model spread. While all models capture a stronger APJ ~~during~~ in EN than in LN

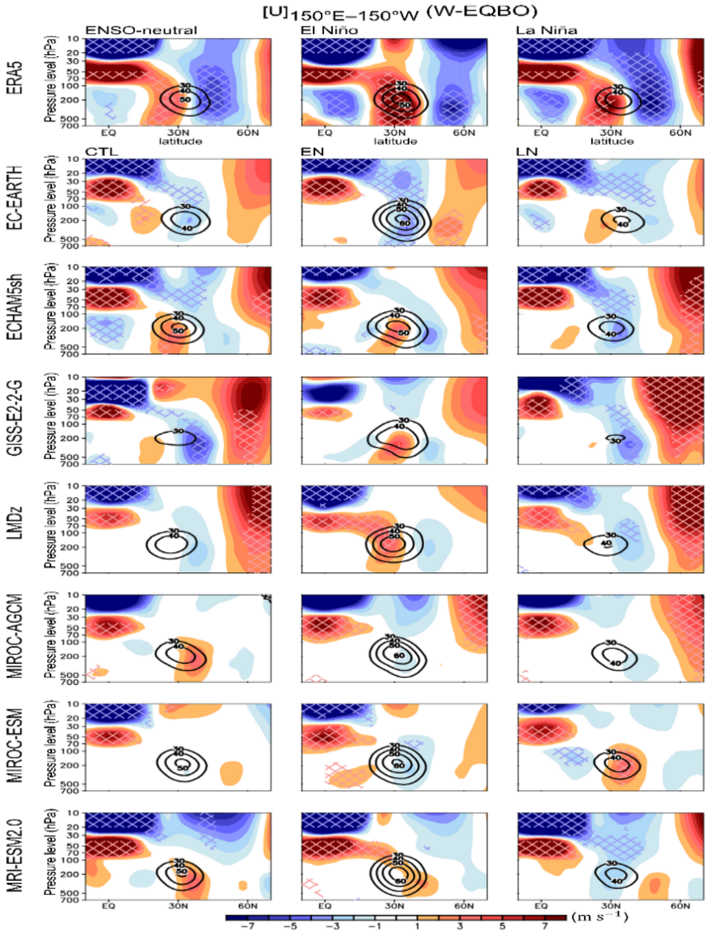

(compare ~~line~~ climatological jet contours in the middle and right columns), they exhibit significant biases in reproducing the ENSO modulation of the QBO~~–~~–APJ connection (filled contours).

Figure 6: QBO-W minus QBO-E composite differences in~~of~~ zonal wind averaged over the Pacific sector (150° E–150° W) during~~for the~~ ENSO-neutral (top-left), El Niño (top-middle), and La Niña (top-right) winters, as well as~~and those~~ in~~for~~ the CTL, EN, and LN experiments (left to right columns). ~~Values that are s~~Statistically significant values at the 95% confidence level are indicated by cross-hatch~~inged~~. The ~~C~~contour denotes the climatological jet, defined as~~with~~ a zonal wind speed ~~equal to or greater than~~≥ 30 m s^{-1}. QBO phases~~QBO-W and QBO-E phases~~ are determined~~defined~~ using~~as~~ deseasonalized February~~–~~–March zonal-mean zonal wind at 70 hPa, averaged over 5°S–5°N ~~at 70 hPa,~~ with~~being~~ > 0.5 σ indicating QBO-W and < −0.5 σ indicating QBO-E~~, respectively~~. The ~~N~~numbers of QBO phase samples (QBO-W, QBO-E) ~~categories for~~in ERA5 are (10, 9) during~~in~~ ENSO-~~N~~neutral, (6, 3) during~~in~~ El Niño, and (12, 7) during~~in~~ La Niña winters.

The inter-model spread of the QBO subtropical ~~route~~pathway is summarized by the APJ-shift index in Fig. 7. Th~~e~~is~~ APJ-shift~~ index is derived from the QBO-W minus QBO-E zonal wind differences shown in Fig. 6. Specifically, it is defined as~~by~~ the 250-hPa QBO zonal wind difference between~~from~~ the northern flank (40°–50° N) and~~to~~ the southern flank (20°–30° N) of the climatological APJ. ~~—~~Negative values indicate ~~that the~~an~~ APJ shifts~~ equatorward shift of the APJ during QBO-W relative~~compared~~ to QBO-E. The observed APJ-shift index is significantly negative during ~~the~~ ENSO-neutral ~~winter~~ (black) and La Niña ~~winter~~ (blue) winters~~,~~ but ~~is~~ insignificant during El Niño (red) winters. This is consistent with dipolar wind anomalies switching sign across the climatological APJ during ENSO-neutral and La Niña winters, whereas~~while the change in~~ APJ strengthening is more pronounced during El Niño winters (~~see~~ Fig. 6). The APJ-shift index is not robust across models. None of the models show a statistically significant APJ shift in response to the QBO, regardless of the ENSO phase. This ~~result~~ suggests that QBOi models substantially~~significantly~~ underestimate or fail to reproduce the subtropical ~~route~~pathway of the QBO teleconnection and its modulation~~modification~~ by ~~the~~ ENSO.

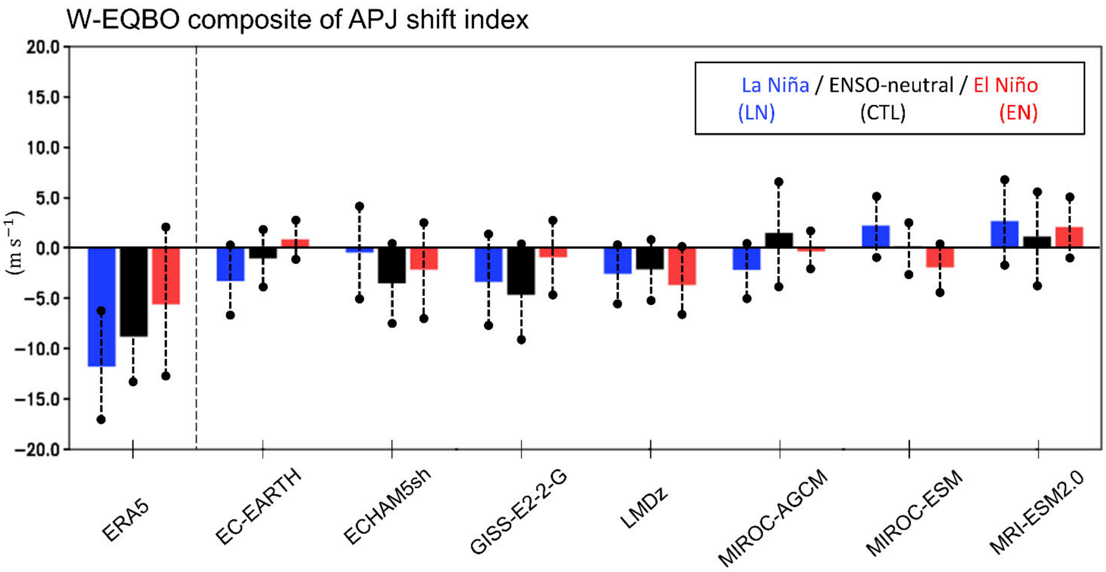

Figure 7: QBO-W minus QBO-E composite differences in~~of~~ the Asia~~-~~–Pacific Jet (APJ) shift index. The APJ-shift index is defined as the difference in~~of~~ the 250-hPa zonal wind anomalies ~~averaged over the Pacific sector (150° E–150° W)~~between the northern flank (40°–50° N) and the southern flank (20° N–30° N) of the climatological APJ core, averaged over the Pacific sector (150° E–150° W). A~~The~~ negative value indicates that the APJ shifts~~moves~~ ~~toward the~~ equatorward during the QBO-W phase. ~~The c~~Composite differences are shown for ~~the~~LN/ La Niña ~~or LN experiment~~ (blue), CTL/ENSO-neutral ~~or CTL~~ (black), and EN/El Niño ~~or EN experiment~~ (red). The APJ shift index~~values~~ is~~are~~ considered significant if the 5–95 % range of the bootstrap distribution (vertical dashed lines) does not include~~encompass~~ zero.

Given that the subtropical jet routepathway of the QBO teleconnection can be influenced by the QBO amplitude and/or the climatological position of the subtropical jet (Garfinkel and Hartmann, 2011a), we examined whether model performance in simulating these two factors is related to the ability of a model to capture the QBO-induced shift of the APJ (Fig. S3). Here, the QBO amplitude is defined as the root--mean square of the deseasonalized zonal--wind time series at 70 hPa, multiplied by $\sqrt{2}$, following Dunkerton and Delisi (1985) and Bushell et al. (2022). The climatological position of the APJ is defined as the latitude of the maximum zonal-mean wind averaged over the APJ sector (150° E–150° W). Consistent with previous studies (Bushell et al., 2022; Anstey et al., 2022c), most QBOi models underestimate the QBO amplitude. Only two models show a comparable QBO amplitude comparable to the reanalysis. However, model biases in the QBO amplitude do not affect those in the QBO–-APJ connection (Fig. S3a). Models with larger QBO amplitudes do not necessarily exhibit stronger jet responses, nor do models with smaller amplitudes consistently show weaker responses. A similar result is also found forin the APJ position (Fig. S3b). These results suggest that neither the QBO amplitude nor the APJ position explains the inter-model spread in the QBO–-APJ connection. Other factors, such as transient and stationary eddies, may determine the QBO–-APJ connection in the models. This possibility shouldneeds to be explored in a future studyies.

5 QBO teleconnections: the tropical routepathway

This section investigates the tropical routepathway of the QBO teleconnection modulated by ENSO, focusing on tropical precipitation and the Walker circulation.

5.1 Tropical precipitation

Several studies have suggestedproposed that the observed QBO signal from the QBO inon tropical precipitation depends on the underlying ENSO phase (e.g., Taguchi et al., 2010;, García--Franco et al., 2022, 2023). This section examinesinvestigates this hypothesis using these QBOi models and experiments through the analyseis of tropical precipitation and OLR. Figure 8 shows the DJF seasonal-mean precipitation differences between QBO-W and QBO-E in EN and LN, together with anomalies duringfor El Niño and La Niña winters fromfor GPCP. In the observations, the QBO signals are strongestlargest and statistically significant in the tropical Pacific and Indian oOceans, consistentand are in good agreement with previous analyses (Liess and Geller, 2012; García-Franco et al., 2022). The positive equatorial Pacific signal in the GPCP dataset, which resembles an El Niño anomaly (Dommenget et al., 2013; Capotondi et al., 2015), is particularly strong and statistically significant duringin DJF. This signal is associated with the three strongest El Niño events (1982–1983, 1997–1998, 2015–2016), coinciding with the westerly QBO phase (Fig. S4; and García-Franco et al., 2023).

Although most models do not reproduceshow such El -Niño–-like precipitation anomaly patterns in either experiment, several models exhibit significant precipitation QBO-related precipitation signals. For example, GISS, ECHAM5sh, and MRI-ESM2.0 show significant QBO responses in the EN experiment, which are comparable in magnitude to the signal diagnosed in GPCP when considering all months (Fig. S5a), thoughbut weaker than the corresponding observed signals underin El Niño and La Niña conditions. However, the response iIn other models, the response is generally weaker, and the spatial distribution of the anomalies is not inconsistent acrossbetween models. In the LN experiments, the models similarlyalso fail to do not show a clear precipitation signal in the Pacific, althoughbut EC-EARTH, ECHAM5sh, WACCM, and MIROC-ESM exhibitshow a responseseveral precipitation signals over the Indian Ocean and Australia. A multi-model mean response is shown in (Fig. S5), which illustrates the lack of model agreement, characterized bywith a virtually zero the mean QBO signal effectively vanishingin a multi-model mean sense across the tropics. Thus, tThis result suggests that there is littlea lack of consensus among models agreement regarding bothin the spatial distribution and the sign of the tropical precipitation response to the QBO phase. Figure S6These results are furtheralso supportsed by Fig. S6 this, which showsing DJF seasonal outgoing longwave radiation (OLR) differences between QBO-W and QBO-E in EN and LN, alongsidetogether with ERA5. None of the models reproduceshow anthe observed OLR signal comparable to observations, and some models (EC-EARTH, ECHAM5sh, LMDz, and GISS) show OLR (and precipitation; Fig. 8) responses that differ appear distinctly between EN and LN experiments, in regions such asespecially over the equatorial Pacific. In summaryother words, there is no robust or consistent or robust precipitation response across models or experiments.

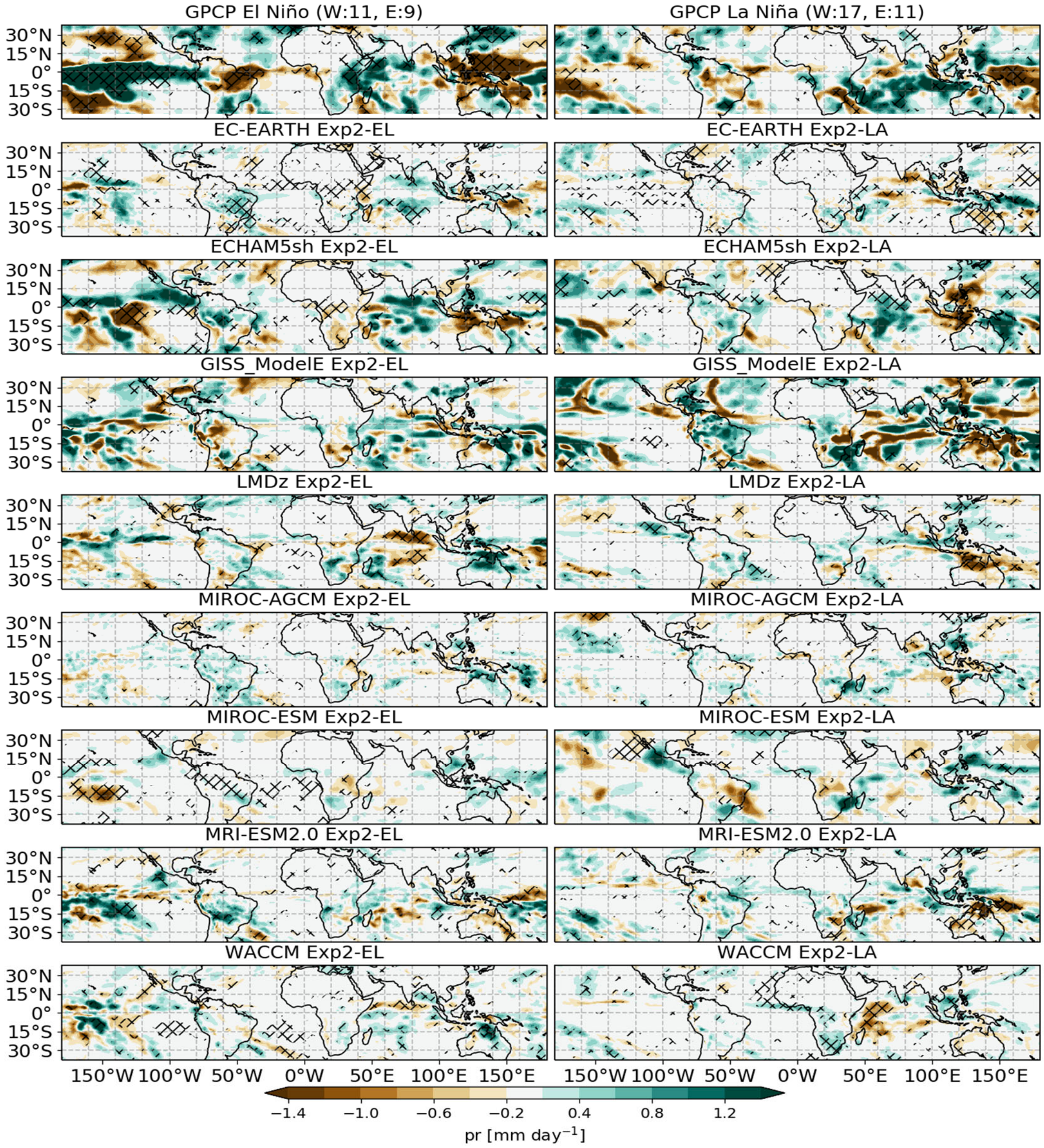

Figure 8: DJF seasonal~~–~~-mean precipitation differences (mm day^{-1}) between ~~(~~QBO-W and~~minus~~ QBO-E~~)~~ for (left) EN and (right) LN experiments in~~for~~ the QBOi models, including El Niño and La Niña winters~~years~~ from~~in~~ GPCP data. Hatching indicates~~denotes~~ statistical significance at the 95% confidence level, determined by~~according to~~ a bootstrap test for ~~the~~ observations and a two-sided t-test for models. ~~The o~~Observed composite sample sizes (in months) are shown in parenthese~~i~~s in the GPCP panels. QBO phases are classified based on~~using~~ deseasonalized DJF~~-~~-mean zonal-mean zonal wind ~~averaged over 5° S–5° N~~ at 50 hPa, averaged over 5° S–5° N, with values~~using~~ ≥ 2 m s^{-1} indicating~~for~~ QBO-W and ≤ −2 m s^{-1} indicating~~for~~ QBO-E.

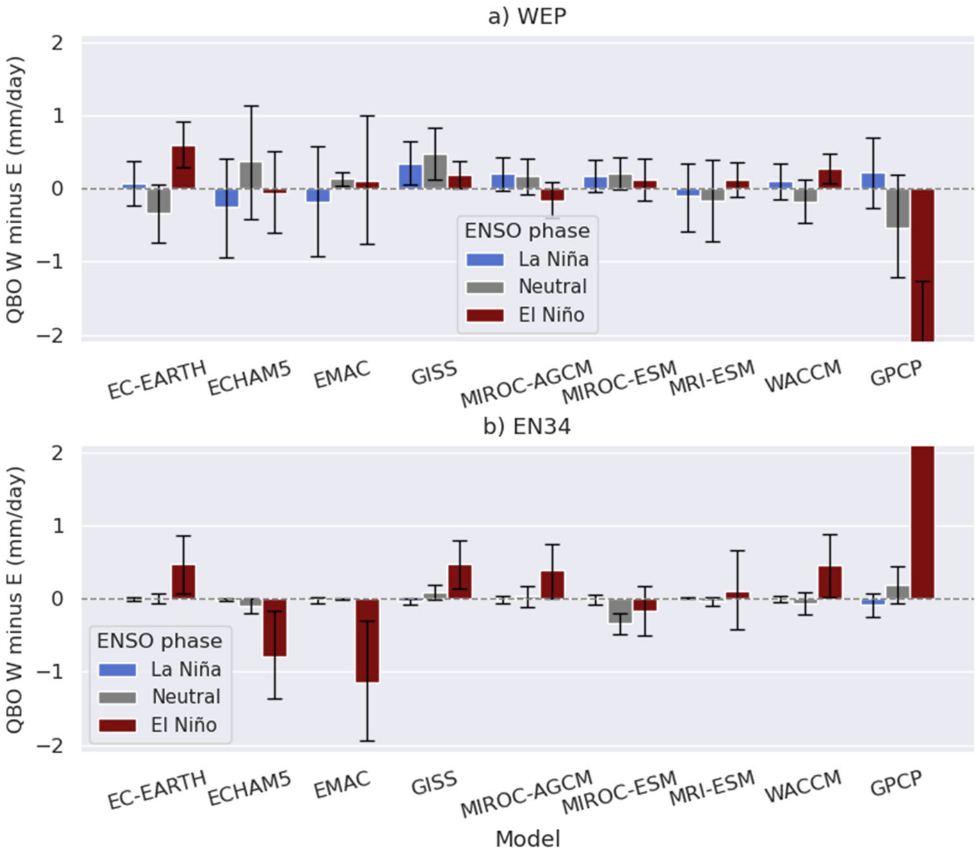

Figure 9: (a-b) Box plots of QBO-W minus QBO-E differences in DJF precipitation (mm day^{-1}) for~~in~~ (a) the western equatorial Pacific (WEP) and (b) the EN3.4 region (5° S–5° N, 170°–120° W). Error bars represent the 95 % confidence interval. ~~Note that t~~The y-axis is fixed for clarity~~to make the plot clearer~~;~~,~~ however,~~but~~ an alternative version with~~where the~~ y-~~-~~axis limits set according to~~are set based on~~ the GPCP scale~~bar~~ is provided in supplementary Fig. S8.

Previous studies have shown that the QBO signal during~~in~~ DJF is particularly strong~~prominent~~ in specific~~particular~~ regions of the tropical Pacific: the western equatorial Pacific (WEP,~~)~~ ~~region (~~5° S–5° N, 120°–170° E) and the Niñ~~n~~o3.4 region (EN3.4, 5° S–5° N, 170°–120° W) (~~EN3.4;~~ Gray et al., 2018;~~,~~ Serva et al., 2022;~~,~~ García-Franco et al., 2022). To test~~examine~~ the ~~extent to which precipitation~~ sensitivity of precipitation in these regions ~~is sensitive~~ to the QBO phase, we analyze~~evaluated~~ the area-averaged precipitation in both regions as a function of QBO and ENSO phases (Fig. S7). The QBOi models show considerable~~significant~~ spread in the ~~their climatology of~~ precipitation climatology~~amounts~~. However,~~but~~ all ~~the~~ simulations ~~seem to~~ reproduce the observed ENSO signal:~~, i.e.,~~ wetter conditions in the EN3.4 region and drier conditions in the WEP in EN, with~~and~~ the opposite pattern in LN, regardless of the QBO phase.

Figure 9 shows the area-averaged precipitation differences (QBO-W minus QBO-E) for the WEP and EN3.4 ~~per~~ regions ~~for the~~ in the CTL, EN, and LN experiments, along with ENSO-~~-(N~~neutral~~)~~, El Niño, and La Niña ~~experiments/~~winters from

GPCP.~~)~~ In observations, the precipitation signal associated with the QBO during El Niño is opposite in sign to that during~~of~~ La Niña. However, these results should be interpreted with caution due to~~One must consider~~ the ~~very~~ small sample size (approximately~~roughly~~ 3–~~to~~ 5 winters in each composite)~~ in these observations when interpreting these results~~. Regardless of the observed sign and magnitude~~ of the observed response~~, the models generally~~seem to show~~ disagree~~ment~~ on the sign of the precipitation response~~, i.e., comparing models~~ in each~~the same~~ experiment~~ provides no consistent precipitation signal~~. For example, while the QBO signal during La Niña ~~response~~ is positive over the WEP in observations and most models agree, only five~~5~~ out of seven~~7~~ models capture~~show~~ this~~a~~ positive response. ~~When looking at individual models,~~ GISS and MIROC-ESM show~~agree that the~~ positive precipitation signals ~~(QBO-W minus QBO-E) is positive~~in the WEP across~~in~~ all ~~their~~ three experiments. However,~~but~~ in the EN3.4 region, none of~~no~~ the models reproduce consistent~~agrees on the sign of the precipitation~~ QBO-related responses across~~in~~ all three experiments~~ for the EN3.4 region~~.

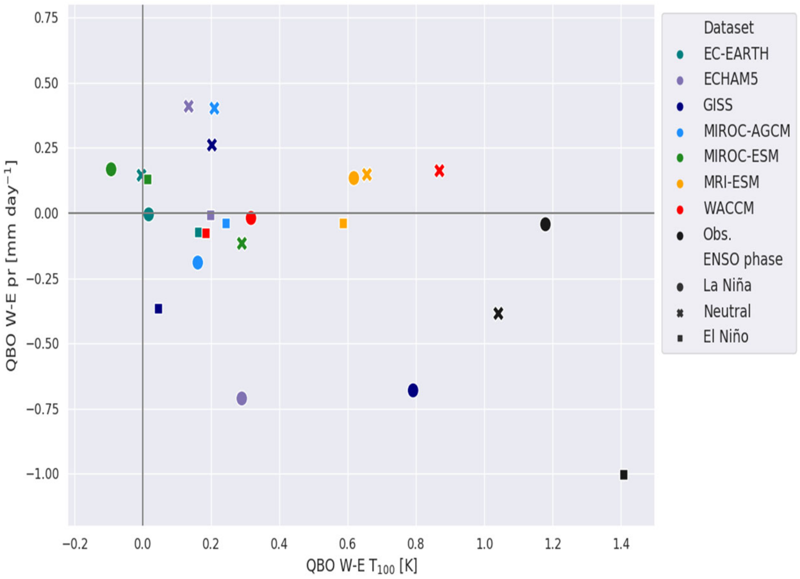

Figure 10: Scatter plot of DJF ~~air~~ temperature differences at 100 hPa (QBO-W minus QBO-E, in K) versus precipitation differences (QBO-W minus QBO-E, in mm day^{-1})~~,~~. ~~B~~both ~~variables were~~ averaged over~~in~~ the western equatorial Pacific region. The correlation coefficient of the best-fit line for all ~~the~~ data, including observations, is −0.48, which is significant at~~to~~ the 95% confidence level according to a t-test. ~~(The correlation~~ W~~w~~ithout observations, the correlation is −0.25.~~)~~ Under El Niño conditions, ~~The~~the correlation ~~coefficient changes when only El Niño conditions~~ is~~are considered (r =~~ −0.82,~~)~~ while~~as well as~~ under~~for~~ La Niña conditions~~experiments~~, it is~~(r =~~ −0.20~~)~~.

One possible reason for the~~this~~ inter-model and~~/or~~ inter-experiment spread in ~~the~~ precipitation response ~~could be~~is variability~~the model spread~~ in QBO-related temperature~~ associated~~ anomalies at the equator, arising~~resulting~~ from the QBO-induced mean meridional circulation and thermal wind balance. The QBO's impact on the tropical tropopause layer (TTL) ~~region~~ is important for its~~the QBO~~ teleconnection via~~in~~ the tropical pathway~~route~~ (Haynes et al., 2021, Hitchman et al., 2021). ~~Here, one~~A common hypothesis is that when~~if~~ a cold QBO anomaly occurs~~lies~~ in the TTL, convection~~ve systems~~ can~~may grow more efficiently,~~ penetrate~~ing~~ to higher~~greater~~ altitudes, locally amplifying the zonal~~-~~mean QBO cold anomaly

(Tegtmeier et al., 2021). Figure 10 shows a scatter plot of the QBO-W minus QBO-E temperature differences of air temperature at 100 hPa versus the precipitation differences (QBO-W minus QBO-E) over the WEP. One might expectcould reasonably question whether models or experiments with a larger TTL temperature signals or static stability tomay also show a strongerlarger precipitation signals in precipitation. In this panel, ERA5 shows larger QBO differences in the W–E TTL temperature signals diagnosed from ERA5 are larger than those of the models, withand are the strongest signals occurring duringfor El Niño winters. Also, Tthe GPCP precipitation signal diagnosed in GPCP is also largest duringin El Niño, possibly due to the coincidence of the strongestlargest El Niño events with the westerly QBO phase. We confirmed an impact of Rremoving thoese strongest El Niño events (1982–1983, 1997–1998, 2015–2016) significantly alterson the GPCP precipitation signal (Fig. S4). It is found that the impact is more dramatic over the all-year composites at the top, in which For the all-winter composites, the Pacific signal dramatically weakensdisappears when excludingnot considering these cases (Fig. S4a, b). DuringIn the El Niño winters, it is only the eastern portion of the Pacific that significantly changes significantly. There are Ssome models, such as GISS and ECHAM5sh, that exhibithave a strong temperature signals, such as GISS and ECHAM5sh, andwhich have a strong negative precipitation signals in LN. However, most models showhave modest positive temperature differences without a clear precipitation signal. Overall, the QBOi models underestimateshow unrealistically weak QBO wind amplitudes in the lower stratosphere (Bushell et al., 2022) and thuscorrespondingly showhave weak TTL temperature anomalies that are too weak in the TTL (Serva et al., 2022), which maycould help explain their weak precipitation signals.

5.2 Walker circulation

In this subsection, we examine whether the a QBO's impact on the Walker circulation can be detected across different ENSO phases. A recent study (Rodrigo et al., 2025) showed that, in reanalyses, the QBO signal in the divergent circulation is strongest over the Maritime Continent region duringin boreal summer (JJA), followed by autumn (SON), and weakest in DJFwinter. However, under El Niño and La Niña conditions, this timing may shift slightly shift, potentially due to the ENSO's influence on the QBO itself (Taguchi, 2010b; Kawatani et al., 2025). Additionally, model diversity and biases in the simulated QBO (Bushell et al., 2022) may contributecould lead to inter-model variations in the simulated QBO teleconnection. We begin ourthe analysis by applying a common QBO definition and target season acrossto all models, using the zonal-mean zonal wind at 70 hPa during JJA to define the QBO phase. With this approach, we identify a coherent signal, characterized by anomalous westerlies in the upper troposphere and anomalous easterlies in the lower troposphere over the Indian Ocean–Maritime Continent region, in both observations and some models acrossin the CTL, LN, and EN experiments (Figures S9, S10, and S11). To strengthenenhance this signal and capture the strongest response in each model, we allow minorslight adjustments to the QBO definition and target season when necessary. The Bonferroni correction (Holm, 1979; see Section 2) is applied to the two-sided t-test when a level or season other than 70 hPa during JJA is used to define the QBO phase.

Figure 11 illustrates~~shows~~ the QBO zonal wind signal averaged over 10° S–10° N in ~~the~~ LN~~ experiment~~, represented by the QBO-W minus QBO-E composite (shading), with ~~the~~ climatological winds superimposed (black contours). In~~Focusing on~~ ERA5 during La Niña (Fig. 11a), the August–~~-~~September–~~-~~October (ASO) climatology~~mean state~~ shows~~features~~ upper-level easterlies over the Eastern Hemisphere and westerlies over the Western Hemisphere, with a weaker, opposite pattern in the lower troposphere. A distinct QBO signal is observed in the equatorial troposphere over the Indian Ocean–Maritime Continent. This

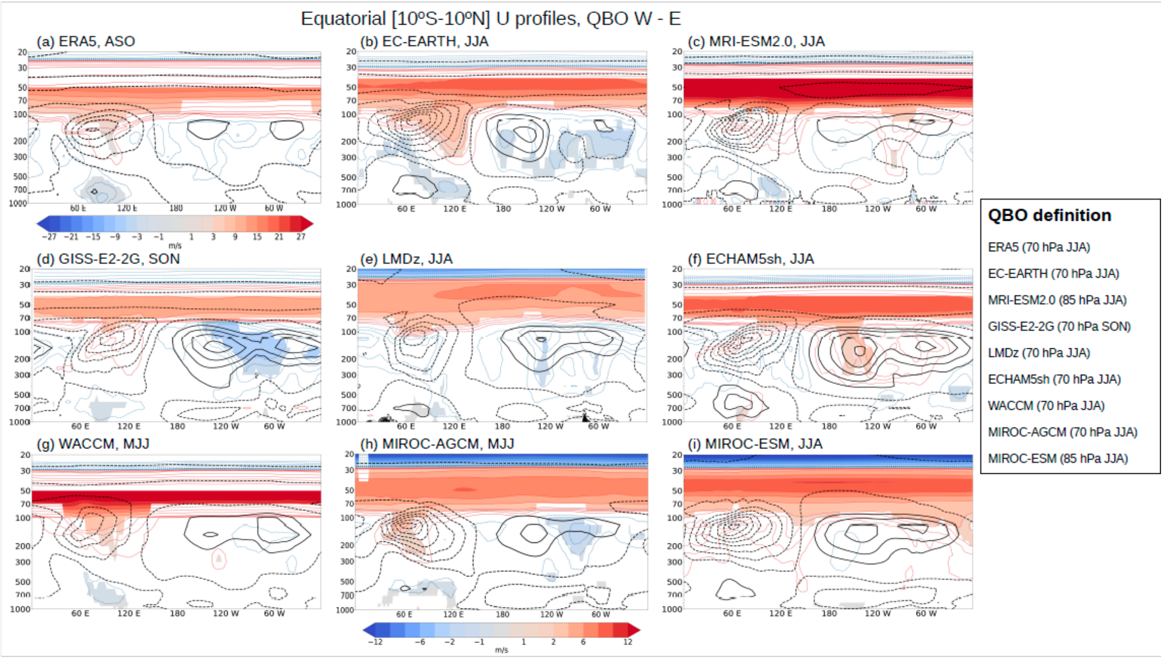

signal is characterized by anomalous westerlies in the upper troposphere (red contours and shading) and anomalous easterlies in the lower troposphere (blue contours and shading). Relative to the climatology, this signal represents a weakening of the ~~mean~~ zonal circulation over the Indian Ocean–Maritime Continent~~ region~~. Similar QBO-related anomalies to those observed in ERA5 for La Niña~~,~~ —featuring upper-level westerlies and lower-level easterlies~~,~~ —are also found in most models in~~for~~ LN experiments (Figs. 11b–~~-~~i), although their precise locations vary~~ies~~ and the lower-level anomalies are generally weaker. Specifically, the strongest signals are found~~identified~~ in EC-EARTH, MRI-ESM2.0, LMDz, and MIROC-AGCM during JJA; GISS during SON; and ~~in~~ WACCM during MJJ. In contrast, ECHAM5sh and MIROC-ESM show~~exhibit~~ no significant signal. The QBO-W minus QBO-E composite in CTL shows a similar signal to that in LN in most models during JJA~~summer~~ or SON~~autumn~~ (Fig. S12). This modulation of the tropical circulation by the QBO appears robust, despite variations~~differences~~ in ~~the~~ timing and longitudinal location.

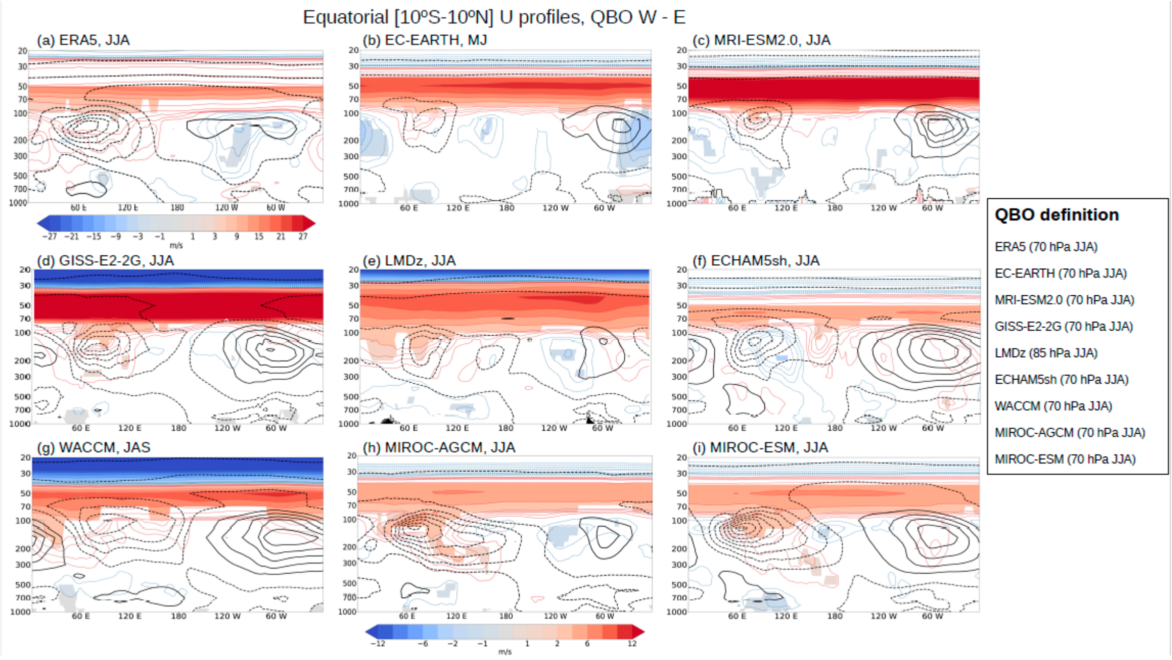

Figure 11: Climatology (black contours) and QBO-W ~~Westerly (W)~~ minus QBO-E~~Easterly (E)~~ differences (shading and colored contours) in equatorial zonal wind profiles, averaged over 10° S–10° N, from the LN experiment for the QBOi models, along with La Niña winters in ERA5. Black contours are drawn at 4 m s^{-1} intervals. Colored contours use the same intervals as the shading, with red contours indicating positive differences and blue contours indicating negative differences. The target season for each panel is indicated in the title, with the QBO definition provided in the legend. ~~In ERA5, 15 La Niña events are identified using the NINO3 index during DJF, and~~QBO phases ~~they~~ are classified based on deseasonalized zonal-mean zonal wind at 70 or 85 hPa in summer and autumn (see the legend), with values ≥ σ (standard deviation) indicating QBO-W and ≤ −σ indicating QBO-E. In ERA5, 16 La Niña events are identified using the NINO3 index during DJF. The numbers of QBO phase categories (QBO-W, QBO-E) in ERA5 are (8, 8) for these events~~into 10 QBO-W and 5 QBO-E categories by analyzing the zonal-mean zonal wind at 50 hPa in summer and autumn~~, with values ≥ 0 m s^{-1} indicating QBO-W and ≤ 0 m s^{-1} indicating QBO-E. Only statistically significant zonal wind differences at the 95 % confidence level are shaded. For models using~~with~~ a QBO definition other than 70 hPa during JJA, the Bonferroni correction is applied (see Section 2). Note that the color bar for ERA5 differs due to~~because of~~ the larger QBO amplitude.

During El Niño in ERA5 (Fig. 12a), the QBO signal in the equatorial troposphere resembles that observed during La Niña, although it occurs during JJA and is weaker. It also shows anomalous westerlies in the upper troposphere over the Indian Ocean–Maritime Continent and anomalous easterlies in the lower troposphere. As in~~for~~ LN, this anomalous zonal circulation indicates~~implies~~ a weakening of the climatological pattern. Comparable anomalies, with~~featuring~~ upper-level westerlies and lower-level easterlies over the same region, are also present in most models. The strongest signals are found~~occur~~ in EC-EARTH during MJ; in MRI-ESM2.0, GISS, LMDz, MIROC-AGCM, and MIROC-ESM during JJA; and in WACCM during JAS. By~~In~~ contrast, ECHAM5sh shows only~~displays~~ a weak response that differs from the other models.

Figure 12: Same as Figure 11, but for EN experiments, along with~~and~~ El Niño events~~years~~ in ERA5. In ERA5, 14 El Niño events are identified, with~~and~~ QBO phase categories (QBO-W, QBO-E) of (7, 7)~~they are classified into 7 QBO-W and 7 QBO-E categories~~.

Figure 13 presents~~shows~~ a summary diagram showing the timing and location of ~~when and where the~~ statistically significant QBO-W minus QBO-E composite differences in equatorial zonal wind (10° S–10° N) ~~occur~~ across all three experiments, ~~illustrating QBO-W minus QBO-E differences~~ at three representative vertical levels (700, 100, and 70 hPa) and over the four standard seasons. These statistically significant signals are identified by analyzing~~examining~~ the influence of the QBO on zonal winds within the longitudinal band from 60° E to~~and~~ 120° E. An example from the EC-EARTH CTL experiment is shown~~provided~~ in Fig. S13. The QBO phase is consistently defined for~~in~~ the specific season indicated in the legend (i.e., it does not vary seasonally). In some models, the strongest signals occur during transitional periods between standard seasons;~~,~~ in such cases,~~so~~ the corresponding symbols are placed accordingly. Across all three experiments, nearly all models, along with ERA5, exhibit a tropospheric signal characterized by upper-level (100 hPa) westerly and lower-level (700 hPa) easterly anomalies during various~~varying~~ seasons from May to November.~~,~~ This pattern suggests~~sing~~ a weakening of the climatological Walker circulation over the Indian Ocean–Maritime Continent. Exceptions include GISS in CTL, MIROC-ESM in CTL and LN, and ECHAM5sh in LN and EN (see Figs. 11, 12, and S12). Overall, this figure illustrates that the QBO, when defined around JJA~~summer~~ and SON~~autumn~~, modulates the zonal circulation in the equatorial troposphere over the Indo–Pacific region. ERA5 shows a consistent signal during both La Niña and El Niño years, which is reproduced by~~in~~ some models with ~~slight~~ variations in season, longitude, or the level used to define the QBO, but is absent~~missing~~ in others. It is important to~~Again, we~~ note that the QBOiENSO experiments are idealized, and ERA5 should not be considered a definitive~~true~~ benchmark.

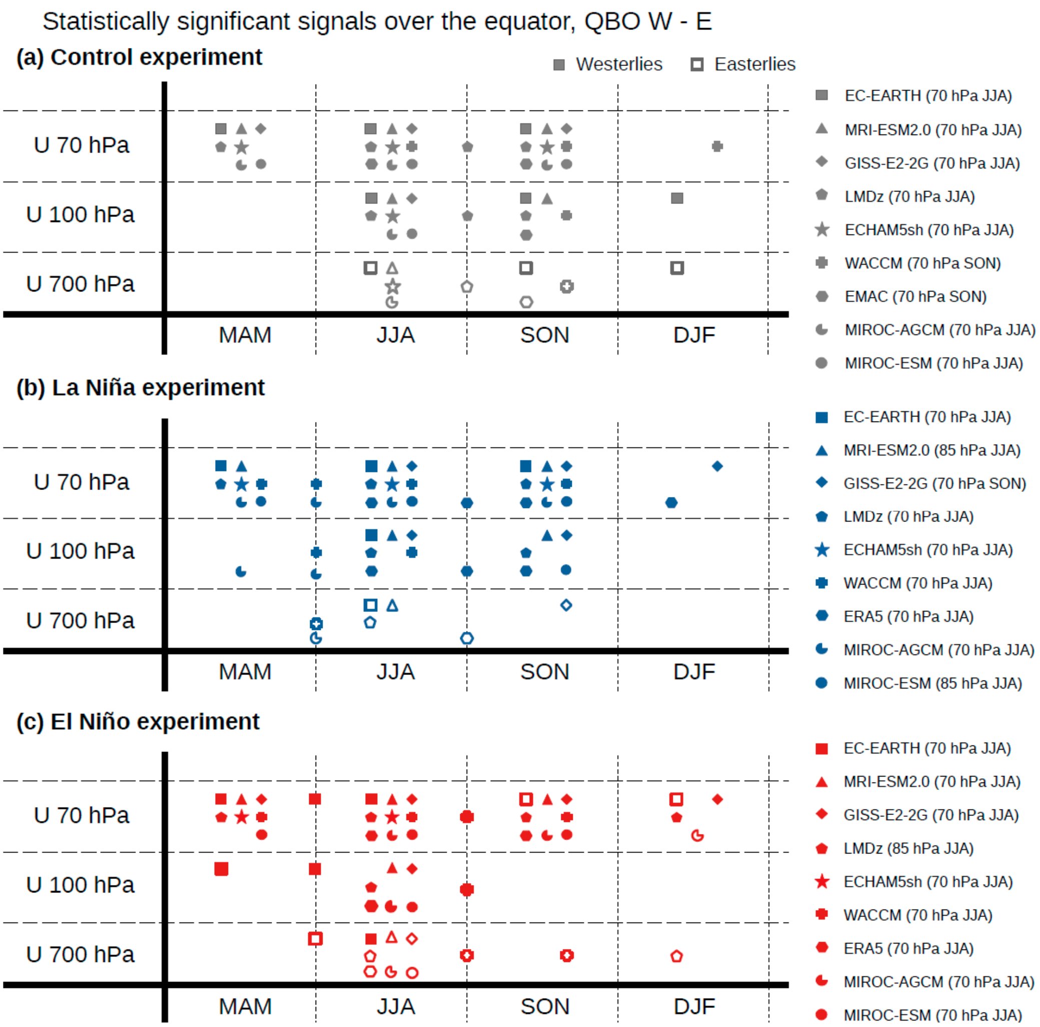

Figure 13: (a) Occurrence of a statistically significant zonal wind signals by models, season, and altitude over the equatorial band (10° S–10° N,) 60° E–120° E) band for the (a) CTL, (b) LN, and (c) EN experiments. The QBO-W minus QBO-E zonal wind signals are evaluated at three vertical levels and across the four standard seasons. Symbols are placed between standard seasons when the strongest signal occurs duringin an intermediate period. Filled symbols represent westerly anomalies, while open symbols indicate easterly anomalies. The QBO definition for each model and experiment is provided in the legend and are the same as Figures 11, 12, and S12.

6 Summary and Discussion

In this paper, we have examinedexamine QBO teleconnections modulated byand ENSO teleconnections in the Arctic stratosphere, the subtropical Pacific jet, and the tropical troposphere. We use Aa multi-model ensemble of QBO-resolving models that performed the QBOiENSO experiments has been used to evaluateexamine the robustness of these teleconnections. Difficulties can arise in Ddistinguishing the respective influences of the QBO and ENSO influences on the extratropics and tropical troposphere can be challenging because ofdue to the observed aliasing between the QBO and ENSOthese phenomena. To address this,Here we have attempted to separate these competing influences by conducting model integrations with annually -repeating, prescribed SSTs that are representativecharacteristic of either strong El Niño or La Niña conditions, thereby simplifying the ENSO forcing compared in comparison withto the diversity of observed ENSO phases. We have reexamined QBO teleconnections to the extratropics and tropics that werepreviously explored in previous QBOi studies (Anstey et al., 2022c; Serva et al., 2022), but now focusing onaddressing combined QBO––ENSO influences using this new QBOi dataset of QBOi idealized ENSO experiments.

The observed strength of correlation coefficients between the 50-hPa equatorial zonal wind and the strength of the polar vortex strength at stratospheric altitudes induring DJF exhibit considerableshows large uncertainty (Fig. 1a). but The models show less uncertainty because of their larger sample sizes (Fig. 1). Some models reproduce weaker correlations for a specific ENSO experiment, consistent with the observations. the confidence intervals clearly exclude zero at most altitudes during La Niña and ENSO-neutral winters, while El Niño response is statistically significant over a smaller altitude range. The models show a smaller uncertainty due to their larger sample sizes (Fig. 1). Some models have weaker correlations for a particular ENSO experiment, similar to the observations. The Holton-TanHolton–Tan relationship in ERA5 indicates thatrepresents the polar vortex isbeing significantly stronger (weaker) under QBO-W (QBO-E) acrossfor all the ENSO phases, with the strongest response occurring induring the La Niña phase. Nearly half of the models simulateexhibit a stronger polar vortex during NH winter under QBO-W for each experiment, consistent with, but much weaker than the observed response, reachingwithin at most a half of the observed amplitude (Fig. 2). The Sseasonal evolution of the QBO in ERA5 revealsindicates a stronger signal in early (late) winter duringfor the El Niño and in late winter during (La Niña)winters. In the LN experiment, two out of nine models capture the observed late-winter response relatively well, while theand others models do not show little or noany response, or even thean opposite responsedirection (Fig. 3).

Major SSWs occur more frequently during both El Niño and La Niña winters than during ENSO-neutral winters in ERA5. Most models show an increased number of events during EN but fail to capture the LN response, suggesting that the QBOi models struggle to reproduce observed SSW statistics (Fig. 4). Major SSW frequencies vary strongly with both QBO and ENSO phases in ERA5, whereas SSW frequencies between QBO-W and QBO-E phases are indistinguishable in the models. These results indicate that polar vortex responses to idealized ENSO forcing in the QBOi models are strong, whereas responses to equatorial QBO phases are relatively weak (Fig. 5) , independently from the level used to define the QBO (50 or 30 hPa).

One may ask if a model-specific equatorial wind level such as 30 hPa can be more efficient for models to reproduce QBO's impact on the polar vortex (the Holton-Tan effect) than the standard 50-hPa equatorial wind that are optimal for observed teleconnections. However, for both 30-hPa and 50-hPa QBO indices most models underestimate equatorial QBOs and they are struggling to reproduce observed polar vortex responses to the QBO. We have examined whether model performance of

QBO amplitude and/or climatological polar night jet strength is related to the ability of model to capture the QBO-induced polar vortex responses. QBO amplitudes at 50 hPa for most models are poor performance, while climatological polar vortices in NH winter can be reproduced with observed strength. This means that unrealistically weak low-level QBO amplitudes can weaken the QBO teleconnections to the polar vortex, as indicated by the previous QBOi multi-model ensemble studies (Richter et al., 2022; Anstey et al., 2022c).

Major SSWs occur frequently during both El Niño and La Niña winters, compared to ENSO-neutral, in ERA5. Most models show more events during EN but they do not catch the LN response, implying that the QBOi models have some trouble in reproducing observed SSWs statistics (Fig. 4). Major SSW frequencies in ERA5 show strong variation with QBO and ENSO phase. QBOi models are characterized by linear distributions between SSW frequencies and the polar vortex strength in NH winters (similar to ERA5) and overall the EN (LN) experiment displays high (relatively low) SSW frequencies (Fig. 5). SSW frequencies between QBO-W and QBO-E are indistinguishable in the models, indicating that polar vortex responses to the idealized ENSO forcing in the QBOi models are strong, while vortex responses to equatorial QBOs are fairly weak.

The APJ cChanges in the APJ in response to the QBO are examinedinvestigated (Figs. 6 and 7), with a focusing on the late winter, when the subtropical jet routepathway is strongest in the observations. Observational dataIn observations, show that the APJ shifts equatorward during QBO-W winters compared with QBO-E winters associated with the QBO westerly anomaly exhibits a distinct horseshoe-shaped pattern extending from the tropical lower stratosphere to the subtropical lower troposphere; , indicating that the APJ shifts equatorward during the QBO-W winter compared to the QBO-E winter. Hhowever, most models underestimate or fail to reproduce thisthe observed QBO–-APJ relationshipconnection. The observed QBO-APJ connection differs between El Niño and La Niña. In observations, as the APJ strengthens over the Pacific sector in response to El Niño, the QBO subtropical wind anomalies become stronger near the APJ center during El Nino while they do not change much during La Niña as the APJ becomes slightly weaker. All models capture a stronger APJ in EN than in LN. The observed APJ shifts equatorward under QBO-W during the ENSO-neutral winter and La Niña winter winters,, but it is is insignificant during El Niño winters. This APJ-shift index is not robust across models. None of the models show a statistically significant shift of the APJ in response to the QBO, regardless of the ENSO phase. -We have also examined whether the subtropical--jet pathwayroute of the QBO teleconnection iscan be influenced by the QBO amplitude and/or the climatological position of the subtropical jet. AlthoughM-most QBOi models underestimate the QBO amplitude, whereas models with larger QBO amplitudes do not necessarily exhibit stronger jet responses, nor do models with smaller amplitudes consistently show weaker responses. This meansmeans that neither the QBO amplitude nor the APJ position explains the inter-model spread in the QBO–-APJ connection. Other factors, such as transient and stationary eddies, likely play a role inmay determineing the QBO–-APJ connection in the model.

The tropical routepathway of the QBO teleconnection modulated by ENSO is examined, focusing on tropical precipitation (Figs. 8–10) and the Walker circulation (Figs. 11–13). In the GPCP dataset,

Tthe positive equatorial Pacific signal with in the GPCP dataset, which resembles an El Niño–like anomaly in thefor QBO-W minus QBO-E differences, is particularly strong and statistically significant duringin DJF., as shown by previous studies that highlight the issue of strong ENSO events coinciding with the westerly phase (García-Franco et al., 2023). Although most of the models do not reproduceshow such El -Niño—-like precipitation anomaly patterns in either the EN or LN experiments, some models (EC-EARTH, ECHAM5sh, WACCM and MIROC-ESM) show significant precipitation signals over the Indian Ocean and Australia (Fig. 8). The precipitation response to the QBO in these experiments varies bydepends on both the model, region, and ENSO phase, withas there is no consistent response acrossbetween the experiments for each model (Fig. 9). For example, the simulated and observed QBO signals in the Niño 3.4 region disagree on the magnitude and sign. To investigateexplore the causes of discrepancies between models andversus observations differences, we analyze the strength of the QBO impact on the TTL region was analyzed, whichas it is considered to be important for the QBO teleconnection alongin the tropical routepathway (Fig. 10). In particular, we verified whether the strength of the temperature anomaly could explain inter-model or inter-experiment differences in the precipitation signals. Overall, the QBOi models producehave too-weak wind amplitudes and too-weak temperature anomalies in the lower stratosphere. , which could help explain the weak precipitation signals.

Several potential biases likely influence the tropical route of QBO teleconnections. Most proposed mechanisms linking the QBO to the tropical surface rely on interactions between the lowermost stratosphere and the uppermost troposphere. A key bias common to many models, including those used in this study, is a weak QBO amplitude in the lower stratosphere, which limits the effectiveness of stratosphere–troposphere coupling processes (Oueslati et al., 2013; Richter et al., 2020; García-Franco et al., 2022, 2023). Additionally, models exhibit persistent tropospheric biases related to tropical convection and precipitation, including biases in the strength and position of the ITCZ, tropical wave activity and unrealistic distributions of rainfall intensity (Oueslati et al., 2013, Norris et al., 2021). These biases typically stem from model parameterizations, notably in convection and cloud microphysics schemes (Hagos et al., 2021, Norris et al., 2021, Zhou et al., 2022). The combination of these stratospheric and tropospheric biases likely weakens the QBO signal reaching the tropical troposphere and contributes to inter-model differences in the magnitude, timing and spatial manifestation of the teleconnection.

The QBO teleconnection to the Walker circulation in reanalyses is strongest in reanalyses over the Indian Ocean–Maritime Continent region duringin boreal summer, followed by autumn, and weakest in winter (Rodrigo et al., 2025). TUnder ENSO conditions, this timing may shift slightly shift, potentially due to ENSO'sthe influence of ENSO on the QBO itself, and . Furthermore, model diversity and biases, as described above, may cause variability inthe simulatinged QBO teleconnections to vary. ThusHere, we identified the strongest signal for each model, by defining the QBO across different seasons (JJA or SON) and vertical levels (85 or 70 hPa). In ERA5, the equatorial troposphere has Aa distinct QBO signal, that is characterized by upper-level westerly and lower-level easterly anomalies, is observed in the equatorial troposphere in ERA5 over the Indian Ocean–Maritime Continent region, which isdoes not have highvery sensitivitye to the ENSO phase. Most models reproduce a similar pattern across all three experiments, although the lower-level anomalies are generally weaker. This modulation of the tropical circulation by the QBO appears spatially consistentrobust, althoughbut its timing varies.

One possible explanation for the more coherent Walker circulation response is that the zonal circulation in the SST-forced simulations is sufficiently similar across models — owing to the SST forcing — that the responses remain relatively consistent. In contrast, other aspects of the response, such as the tropical precipitation, the polar vortex, and the subtropical jet, may be less constrained by the experimental setup. It is also plausible that the mechanisms driving the Walker cell response are better represented in these models. Given the relatively large static stability anomaly shown in the results (Fig. 10), one could reasonably suspect that this mechanism is strong enough in the models to produce a consistent response in the Walker circulation.

We now consider three issues related toabout modellling the complexity of QBO–-ENSO interactioncomplexity raised by these results: forced SSTs, the seasonality and variabilityvariation of the Walker circulation, and biases in the QBO and other processesdiagnostics.

First, tAMIP-type experiments, where idealized SST patterns and fixed external forcings are used, have been used here to examine QBO-ENSO teleconnections although it is noted that we do not have an observational verification for these experiments. However, the responses of the climate system's response to ENSO forcing tends to be nonlinear with respect to ENSO intensity and asymmetric with respect to ENSOthe phasespolarity of ENSO (Domeisen et al., 2019; Rao and Ren, 2016b, c). This nonlinearity complicates the identification ofmeans that it is difficult to isolate physically meaningful mechanisms and limitsfrom such a nonlinear system and gain understanding ofscientific insights into QBO–-ENSO teleconnections. Therefore, cConducting idealized experiments, such as our QBOiENSO experiments, c that take into account the ENSO-QBO diversity could help us to further clarify physically robustelucidate scientifically meaningful mechanisms within thisin such a complex system. The experimental design of QBOiENSO (Kawatani et al., 2025) is annually repeating, using inflated monthly mean ENSO anomalies from the climatology. However, most QBOi models in the three experiments (CTL, EN, and LN) fail to reproduce QBO-related, El Niño–like precipitation anomalies as observed in the GPCP dataset, whereas such precipitation patterns are captured by some QBOi models in QBOi Experiment 1 of the AMIP-type with interannually varying SSTs (Serva et al., 2022) and by other models in AMIP-type experiments (García-Franco et al., 2022). It is noted that the experimental design of QBOiENSO (Kawatani et al., 2025) is annually locked with monthly-mean anomalies from the climatology. For example, the precipitation responses to the QBO for the AMIP-type experiments with interannually varying SSTs(Serva et al., 2022; García-Franco et al., 2022)

(Serva et al., 2022; García-Franco et al., 2022) is different from those for the QBOi ENSO experiments with perpetual SSTs. The precipitation response to the QBO in the equatorial Pacific signal in the GPCP dataset shows a statistically significant, El-Niño-like anomaly pattern. Most of the models do not show such El-Niño-like precipitation anomaly patterns in the CTL, EN or LN experiments, while such patterns were seen in some of the QBOi models in the QBOi Experiment 1 (Serva et al., 2022). This suggests that the QBO's downward influence on tropical precipitation may be overly sensitive to model physics or muted by the absence of SST feedbacks (García-Franco et al., 2023; Randall et al., 2024), or affected by biases in climatological winds and precipitation characteristics. making it difficult to detect with confidence.

The lack of a robust and coherent QBO related precipitation signal across experiments and models highlights significant spread in how convection and circulation respond to a QBO forcing. This raises the possibility that the QBO's downward impact on tropical precipitation is too sensitive to model physics, or is perhaps muted by the lack of SST feedbacks (García-Franco et al., 2023, Randall et al., 2024) to be clearly detected.

Next, One of the most important points from this study is that Walker circulation would potentially play an important role in tropical teleconnections as well as extratropical teleconnections. We are interested in two distinct and documented El Niño patterns, Eastern Pacific (EP) versus Central Pacific (CP, or Modoki) El Niños, which make a large difference in the Hadley and Walker circulations and also have markedly different impacts on remote regions. One may doubt that weaker ENSO events or different ENSO flavors than those used in this study would yield further insights due to such ENSO events being associated with less dramatic changes in the location of tropical convection. However, the tropical SSTs in the Central Pacific substantially influences the QBO on decadal timescales (Shibata and Naoe, 2022). Thus, such idealized experiments forced with ENSO SST patterns would be beneficial for us to better achieve the changing impact of ENSO events on the QBO teleconnections. We are also interested in tropical convection being inherently coupled with the ocean. Long-term simulations from coupled global circulation models (CGCMs) would be a convenient tool for testing responses of QBO-ENSO teleconnections associated with internal variability of the ocean-atmosphere coupled system (García-Franco et al., 2023; Randall et al., 2023).

Wwe emphasizehave to underline the importance of seasonality infor shaping the combined effects of the QBO- and ENSO on the tropical troposphere. Our results indicatesuggest that QBO teleconnections with the Walker circulation varyexhibit seasonally variability and display a distinct zonally asymmetric pattern. These findings underscoreemphasize the need for further investigation to clarifyelucidate the drivers of thisthe seasonal dependence, the causesnature of the asymmetry, and the underlying mechanisms governing these interactions. We also note that tropical convection is inherently coupled with the ocean. Long-term simulations with coupled general circulation models (CGCMs) would provide a useful framework for testing QBO–ENSO teleconnections arising from internal variability of the coupled ocean–atmosphere system (García-Franco et al., 2023; Randall et al., 2023).

Finally, common systematic model biases hinder QBO teleconnections to both the extratropics and the tropical troposphere. In the extratropical stratosphere, the previous studies usingof QBOi models have suggested that the systematic weakness of the QBO- polar vortex coupling arisein the models might arise from consistentlysystematically weak QBO amplitudes at lower levels in the equatorial stratosphere, biases in the wintertime polar vortex biases in winter, and inadequate representation of stratosphereic - troposphere coupling, etc. (Bushell et al., 2022; Richter et al., 2022; Anstey et al., 2022c). Our results confirm that these unrealistically weak low-level QBO amplitudes reduce the QBO teleconnections with both the polar vortex and the APJ.

. In our QBOiENSO experiments, such systematic model biases were also found because most of the modes were the same as the previous studies. In the tropics, models commonly exhibit weak QBO amplitudes in the lower stratosphere, which limit the effectiveness of stratosphere–troposphere coupling processes (Oueslati et al., 2013; Richter et al., 2020; García-Franco et al., 2022, 2023). Unrealistic variability also emerges in QBOiENSO experiments, with occasional stalling of simulated QBOs (Kawatani et al., 2025). Additionally, persistent tropospheric biases related to tropical convection and precipitation are evident, including biases in the strength and position of the ITCZ, tropical wave activity, and unrealistic rainfall distributions. These shortcomings typically stem from model parameterizations, particularly those governing convection and cloud microphysics (Oueslati et al., 2013; Hagos et al., 2021; Norris et al., 2021; Zhou et al., 2022). The combination of these stratospheric and tropospheric biases likely weakens the QBO signal in the tropical troposphere and contributes to inter-model differences in the magnitude, timing, and spatial manifestation of the teleconnection.

~~In the tropics, our results suggested that the systematic bias of the QBO impact on the tropical troposphere might arise from the systematically weak QBO amplitudes at lower levels, precipitation bias, and inadequate representation of the Walker circulation. Thus, the combination of several biases could be the reason why we have not seen a consistent signal of QBO teleconnections across the models and experiments. Therefore, it is plausible that consistency with observations will not improve without correcting such model biases. Currently, a~~ Phase 2~~project~~ of the QBOi project ~~Phase 2~~ is currently underway~~in progress~~ to assess the impact of QBO biases ~~by~~ using zonal-mean nudging~~ed~~ toward observations in the QBO region. Bias-corrected QBO amplitudes~~,~~ achieved through nudging ~~methods,~~ may provide valuable insights for improving the representation of QBO teleconnections in~~to~~ both the extratropics and the tropical troposphere.

Data availability. The QBOi data archive was hosted by the Centre for Environmental Data Analysis (CEDA), UK, and data processing was performed on the JASMIN infrastructure. ~~The~~ ERA5 reanalysis data can be available~~be obtained~~ from the ECMWF website (https://www.ecmwf.int/en/forecasts/datasets/browse-reanalysis-datasets). The El Niño Monitoring Index (NINO.3) was obtained~~derived~~ from ~~an ENSO monitoring site of~~ the Japan Meteorological Agency's ENSO monitoring site (https://ds.data.jma.go.jp/tcc/tcc/products/elnino/index.html). ~~The~~ GPCP v2.3 data were~~was~~ downloaded from https://doi.org/10.7289/V56971M6 (Adler et al., 2016).

Author contribution. YK, KH, JA, and JHR designed the QBOi~~-~~ENSO–QBO experiments. FS, HN, KY, TK, SW, YK, JGS, FMP, PAB, FL, CO, JHR, and CCJ generated~~created~~ the model-experiment~~ed~~ data and uploaded them to ~~the~~ CEDA. HN, JLGF, CHP, MR, FMP, FS, and MT conducted the analyses, prepared the figures, and contributed to the manuscript. JA, JGS, SWS, NB, and SO contributed to~~in~~ the interpretation of the results. The first draft of the manuscript was prepared by HN, with input from ~~who involved~~all authors on~~for~~ the final version.

Competing interests. The authors declare ~~that they have~~ no conflict of interest.

Acknowledgements. The Editor, Dr. Battisti, and two anonymous referees provided detailed and substantive reviews of the manuscript. Their efforts are greatly appreciated by the authors and contributed substantially to improving the final version. All authors acknowledge ~~the~~ CEDA~~,~~ for~~which~~ kindly host~~ed~~ing the QBOi data archive. ~~-~~HN was supported by MEXT, JSPS KAKENHI (grant numbers~~:~~ JP22H04493, JP24K07140); HN and KY were supported by JSPS KAKENHI JP24K00710. YK was supported by JSPS KAKENHI (JP22K18743) and by the Environment Research and Technology Development Fund (JPMEERF20242001) of the Environmental Restoration and Conservation Agency, provided by Ministry of the Environment of Japan. YK and SW were supported by JSPS KAKENHI (JP22H01303 and JP23K22574). SW was also supported by the MEXT ~~-~~Program for ~~the~~ ~~a~~Advanced ~~s~~Studies of ~~c~~Climate ~~c~~Change ~~p~~Projection (SENTAN) Grant Number JPMXD0722681344. ~~The n~~Numerical simulations with the~~of~~ MIROC models were performed on~~using~~ the Earth Simulator. CP and SS were funded by the Korea Meteorological Administration Research and Development Program ~~under Grant~~ (RS-2025-02307979). MR was supported by the 'Ayudas para la Formación de Profesorado Universitario' programme (FPU20/03517).~~,~~ FMP was supported by the EU/HORIZON-funded MSCA-IF-GF SD4SP project (GA 101065820).~~,~~ ~~and~~ JGS acknowledges funding from the Spanish DYNCAST project (CNS2022-135312). The ECHAM5sh simulations were made possible~~performed~~ thanks to an ECMWF Special Project awarded to FS. NB was funded by the Met Office Climate Science for Service Partnership (CSSP) China project under the International Science Partnerships Fund (ISPF). The AI program ChatGPT was used to refine the language in portions of the final draft. The manuscript does not contain any extended passages written by the AI program.

Review statement. This paper was edited by xxx and reviewed by xxx referees.

References

Adler, R. F., Huffman, G. J., Chang, A., Ferraro, R., Xie, P.-P., Janowiak, J., Rudolf, B., Schneider, U., Curtis, S., Bolvin, D., Gruber, A., Susskind, J., Arkin, P., and Nelkin, E.: The Version-2 Global Precipitation Climatology Project (GPCP) monthly precipitation analysis (1979–present), J. Hydrometeorol., 4, 1147–1167, https://doi.org/10.1175/1525-7541(2003)004<1147:TVGPCP>2.0.CO;2, 2003.

Adler, R., Wang, J. J., Sapiano, M., Huffman, G., Chiu, L., Xie, P.~~-~~-P., Ferraro, R., Schneider, U., Becker, A., Bolvin, D., Nelkin, E., Gu, G., and NOAA CDR Program: Global Precipitation Climatology Project (GPCP) Climate Data Record (CDR), Version 2.3 (Monthly), National Centers for Environmental Information, https://doi.org/10.7289/V56971M6, 2016.

Anstey, J. A., and Shepherd, T. G.: High-latitude influence of the quasi-biennial oscillation, Q. J. R. Meteorol. Soc., 140, 1–21. http://doi.org~~wiley.com~~/10.1002/qj.2132, 2014.

Anstey, J. A., Butchart, N., Hamilton, K., and Osprey, S. M.: The SPARC quasi-biennial oscillation initiative, Q. J. R. Meteorol. Soc., 148, 1455–1458, https://doi.org/10.1002/qj.3820, 2022a.

Anstey, J. A., Osprey, S. M., Alexander, J., Baldwin, M. P., Butchart, N., Gray, L., Kawatani, Y., and Richter, J. H.: Impacts, processes and projections of the quasi-biennial oscillation, Nat. Rev. Earth Environ., 3, 588–603, https://doi.org/10.1038/s43017-022-00323-7, 2022b.

Anstey, J. A., Simpson, I. R., Richter, J. H., Naoe, H., Taguchi, M., Serva, F., Gray, L. J., Butchart, N., Hamilton, K., Osprey, S., Bellprat, O., Braesicke, P., Bushell, A. C., Cagnazzo, C., Chen, C.-C., Chun, H.-Y., Garcia, R. R., Holt, L., Kawatani, Y., Kerzenmacher, T., Kim, Y.-H., Lott, F., McLandress, C., Scinocca, J., Stockdale, T. N., Versick, S., Watanabe, S., Yoshida, K., and Yukimoto, S.: Teleconnections of the quasi-biennial oscillation in a multi-model ensemble of QBO-resolving models, Q. J. R. Meteorol. Soc., 148, 1568–1592. https://doi.org/10.1002/qj.4048, 2022c.

Baldwin, M. P., Gray, L. J. ~~Gray~~, Dunkerton, T. J., Hamilton, K., Haynes, P. H., Randel, W. J., Holton, J. R., Alexander, M. J., Hirota, I., Horinouchi, T., Jones, D. B. A., Kinnersley, J. S., Marquardt, C., Sato, K., and Takahashi, M.: The quasi-biennial oscillation, Rev. Geophys., 39, 179–229, https://doi.org/10.1029/1999RG000073, 2001.

Boer, G. J., Hamilton, K.; QBO influence on extratropical predictive skill, Clim. Dyn., 31, 987–1000, https://doi.org/10.1007/s00382-008-0379-5, 2008.

Bushell, A.C., Anstey, J. A., Butchart, N., Kawatani, Y., Osprey, S. M., Richter, J. H., Serva, F., Braesicke, P., Cagnazzo, C., Chen, C.-C., Chun, H.-Y., Garcia, R. R., Gray, L. J., Hamilton, K., Kerzenmacher, T., Kim, Y.-H., Lott, F., McLandress, C., Naoe, H., Scinocca, J., Smith, A. K., Stockdale, T. N., Versick, S., Watanabe, S., Yoshida, K., and Yukimoto, S.: Evaluation of the ~~Q~~quasi-~~B~~biennial ~~O~~oscillation in global climate models for the SPARC QBO-initiative, Q. J. R. Meteorol. Soc., 148, 1459–1489, https://doi.org/10.1002/qj.3765, 2022.

Butchart, N., Anstey, J. A., Hamilton, K., Osprey, S., McLandress, C., Bushell, A. C., Kawatani, Y., Kim, Y.-H., Lott, F., Scinocca, J., Stockdale, T., Bellprat, O., Braesicke, P., Cagnazzo, C., Chen, C.-C., Chun, H.-Y., Dobrynin, M., Garcia, R. R., García-Serrano, J., Gray, L. J., Holt, L., Kerzenmacher, T., Naoe, H., Pohlmann, H., Richter, J. H., Scaife, A. A., Schenzinger, V., Serva, F., Versick, S., Watanabe, S., Yoshida, K., and Yukimoto, S.: Overview of experiment design and comparison of models participating in phase 1 of the SPARC Quasi-Biennial Oscillation initiative (QBOi), Geosci. Model Dev., 11, 1009–1032, https://doi.org/10.5194/gmd-11-1009-2018, 2018.

Butler, A., and Polvani, L.: El Niño, La Niña, and stratospheric sudden warmings: Reevaluation in light of the observational record, Geophys. Res. Lett., 38, L13807, https://doi.org/10.1029/2011GL048084, 2011.

Butler, A., Seidel, D. J., Hardiman, S. C., Butchart, N., Birner, T., and Match, A.: Defining sudden stratospheric warmings, Bull. Am~~er~~. Meteorol. Soc., 96, 1913–1928, https://doi.org/10.1175/BAMS-D-13-00173.1, 2015.

Butler, A. H., and Polvani, L. M.: El Niño, La Niña, and stratospheric sudden warmings: A reevaluation in light of the observational record, Geophys. Res. Lett., 38, L13807, https://doi.org/10.1029/2011GL048084, 2011.

Butler, A. H., Polvani, L. M., and Deser, C.: Separating the stratospheric and tropospheric pathways of El Niño–Southern Oscillation teleconnections, Environ. Res. Lett., 9, 024014, DOI 10.1088/1748-9326/9/2/024014, 2014.

Butler, A. H., Seidel, D. J., Hardiman, S. C., Butchart, N., Birner, T., and Match, A.: Defining sudden stratospheric warmings, Bull. Am. Meteor. Soc., 96, 1913–1928, https://doi.org/10.1175/BAMS-D-13-00173.1, 2015.

Calvo, N., Giorgetta, M. A., Garcia-Herrera, R., and Manzini, E.: Nonlinearity of the combined warm ENSO and QBO effects on the Northern Hemisphere polar vortex in MAECHAM5 simulations, J. Geophys. Res., 114, D13109, https://doi.org10.1029/2008JD011445, 2009.

Camp, C. D., and Tung, K. K.: Stratospheric polar warming by ENSO in winter: A statistical study, Geophys. Res. Lett., 34, L04809,~~.~~ https://doi.org/10.1029/2006GL028521, 2007.

Capotondi, A., and Sardeshmukh, P. D.: Optimal precursors of different types of ENSO events, Geophys. Res. Lett., 42, 9952–9960, https://doi.org/10.1002/2015GL066171, 2015.

Charlton, A. J., and Polvani, L. M.: A new look at stratospheric sudden warmings. Part I: Climatology and modeling benchmarks, J. Clim., 20, 449–469, https://doi.org/10.1175/JCLI3996.1, 2007.

Collimore, C. C., Martin, D. W., Hitchman, M. H., Huesmann, A., and Waliser, D. E.: On the relationship between the QBO and tropical deep convection, J. Clim., 16, 2552–2568, https://doi.org/10.1175/1520-0442(2003)016<2552:OTRBTQ>2.0.CO;2, 2003.

Crooks, S. A., and Gray, L. J.: Characterization of the 11-year solar signal using a multiple regression analysis of the ERA-40 dataset, J. Clim., 18, 996–1015, https://doi.org/10.1175/JCLI-3308.1, 2005.

Domeisen, D. I., Garfinkel, C. I., and Butler, A. H.: The teleconnection of El Niño Southern Oscillation to the stratosphere, Rev. Geophys., 57, 5–47, https://doi.org/10.1029/2018rg000596, 2019.

Dommenget, D., Bayr, T., and Frauen, C.: Analysis of the nonlinearity in the pattern and time evolution of El Niño Southern Oscillation, Clim. Dyn~~am.~~., 40, 2825–2847, https://doi.org/10.1007/s00382-012-1475-0, 2013.

Dunkerton, T. J.. and Delisi, D. P.: Climatology of the equatorial lower stratosphere, J. Atmos. Sci., 42, 376–396, 1985.

Elsbury, D., Serva, F., Caron, J., Back, S.-Y., Orbe, C., Richter, J., Anstey, J. A., Bretonniere, P.-A., Butchart, N., Chen, C.-C., Garcia-Serrano, J., Glanville, A., Kawatani, Y., Kerzenmacher, T., Lott, F., Naoe, H., Osprey, S., Palmeiro, F. M., Son, S.-W., Taguchi, M., Versick, S., Watanabe, S., and Yoshida, K.: QBOi El Niño Southern Oscillation experiments: Assessing relationships between ENSO, MJO, and QBO, EGUsphere [preprint], https://doi.org/10.5194/egusphere-2024-3950, Weather ~~and~~ Clim.~~ate~~ Dynam.~~ics~~ Discuss.~~ions~~, 2025.

Eyring, V., Bock, L., Lauer, A., Righi, M., Schlund, M., Andela, B., Arnone, E., Bellprat, O., Brötz, B., Caron, L.-P., Carvalhais, N., Cionni, I., Cortesi, N., Crezee, B., Davin, E. L., Davini, P., Debeire, K., de Mora, L., Deser, C., Docquier, D., Earnshaw, P., Ehbrecht, C., Gier, B. K., Gonzalez-Reviriego, N., Goodman, P., Hagemann, S., Hardiman, S., Hassler, B., Hunter, A., Kadow, C., Kindermann, S., Koirala, S., Koldunov, N., Lejeune, Q., Lembo, V., Lovato, T., Lucarini, V., Massonnet, F., Müller, B., Pandde, A., Pérez-Zanón, N., Phillips, A., Predoi, V., Russell, J., Sellar, A., Serva, F., Stacke, T., Swaminathan, R., Torralba, V., Vegas-Regidor, J., von Hardenberg, J., Weigel, K., and Zimmermann, K.: Earth System Model Evaluation Tool (ESMValTool) v2.0 — an extended set of large-scale diagnostics for quasi-operational and comprehensive evaluation of Earth system models in CMIP, Geosci. Model Dev., 13, 3383–3438, https://doi.org/10.5194/gmd-13-3383-2020, 2020.

García-Franco, J. L., Gray, L. J., Osprey, S., Chadwick, R., and Martin, Z.: The tropical route of quasi-biennial oscillation (QBO) teleconnections in a climate model, Weather Clim. Dynam., 3, 825–844. https://doi.org/10.5194/wcd-3-825-2022, 2022.

García-Franco, J. L., Gray, L. J., Osprey, S., Jaison, A. M., Chadwick, R., and Lin, J.: Understanding the mechanisms for tropical surface impacts of the quasi-biennial oscillation (QBO), J. Geophys. Res., 128, e2023JD038474, https://doi.org/10.1029/2023JD038474, 2023.

García-Serrano, J., Cassou, C., Douville, H., Giannini, A., and Doblas-Reyes, F. J.: Revisiting the ENSO teleconnection to the tropical North Atlantic, J. Clim., 30, 6945–6957, https://doi.org/10.1175/JCLI-D-16-0641.1, 2017.

Garfinkel, C. I., and Hartmann, D. L.: Effects of the El Niño–Southern Oscillation and the Quasi-Biennial Oscillation on polar temperatures in the stratosphere, J. Geophys. Res., 112, D19112,~~.~~ https://doi.org/10.1029/2007JD008481, 2007.

Garfinkel, C. I., and Hartmann, D. L.: Different ENSO teleconnections and their effects on the stratospheric polar vortex, J. Geophys. Res., 113, D18114,~~.~~ https://doi.org/10.1029/2008JD009920, 2008.

Garfinkel, C. I., and Hartmann, D. L.: The influence of the quasi-biennial oscillation on the troposphere in winter in a hierarchy of models. Part I: Simplified dry GCMs, J. Atmos. Sci., 68, 1273–1289, https://doi.org/10.1175/2011JAS3665.1, 2011a.

Garfinkel, C. I., and Hartmann, D. L.: Influence of the quasi-biennial oscillation on the troposphere in winter in a hierarchy of models. Part II: perpetual winter WACCM runs, J. Atmos. Sci., 68, 2026–2041, https://doi.org/10.1175/2011JAS3702.1, 2011b.

Garfinkel, C. I., Butler, A. H., Waugh, D. W., Hurwitz, M. M., and Polvani, L. M.: Why might stratospheric sudden warmings occur with similar frequency in El Niño and La Niña winters?, J. Geophys. Res., 117, D19106, https://doi.org/10.1029/2012JD017777, 2012a.

Garfinkel, C. I., Shaw, T. A., Hartmann, D. L., and Waugh, D. W.: Does the Holton-Tan mechanism explain how the quasi-biennial oscillation modulates the Arctic polar vortex?, J. Atmos. Sci., 69, 1713–1733, https://journals.ametsoc.org/doi/10.1175/JAS-D-11-0209.1, 2012b.

Garfinkel, C. I., Schwartz, C., Domeisen, D. I. V., Son, S.-W., Butler, A. H., and White, I. P.: Extratropical atmospheric predictability from the ~~Q~~quasi-~~B~~biennial ~~O~~oscillation in subseasonal forecast models, J. Geophys. Res., 123, 7855–7866,~~.~~ https://doi.org/10.1029/2018JD028724, 2018.

Gray, L. J., Anstey, J. A., Kawatani, Y., Lu, H., Osprey, S., and Schenzinger, V.: Surface impacts of the Quasi Biennial Oscillation, Atmos. Chem. Phys., 18, 8227–8247, https://www.atmos-chemphys.net/18/8227/2018/, 2018.

Gray, W. M., Scheaffer, J. D., and Knaff, J. A.: Influence of the stratospheric QBO on ENSO variability, J. Meteor. Soc. Japan, 70, 975–995, https://doi.org/10.2151/jmsj1965.70.5_975, 70, 975–995, 1992.

Hagos, S. M., Leung, L. R., Garuba, O. A., Demott, C., Harrop, B., Lu, J., and Ahn, M. S.: The relationship between precipitation and precipitable water in CMIP6 simulations and implications for tropical climatology and change, J. Clim., 34, 1587–1600, https://doi.org/10.1175/JCLI-D-20-0243.1, 2021.

Hansen, F., Matthes, K., and Wahl, S.: Tropospheric QBO-ENSO interactions and differences between the Atlantic and Pacific, J. Clim., 29, 1353–1368, https://doi.org/10.1175/JCLI-D-15-0164.1, 2016.

Haynes, P., Hitchcock, P., Hitchman, M., Yoden, S., Hendon, H., Kiladis, G., Kodera, K., and Simpson, I.: The influence of the stratosphere on the tropical troposphere, J. Meteorol. Soc. Japan. Ser. II, 99, 803–845, https://doi.org/10.2151/jmsj.2021-040, 2021.

Hersbach, H., Bell, B., Berrisford, P., Hirahara, S., Horáanyi, A. Muñnoz-Sabater, J., Nicolas, J., Peubey, C., Radu, R., Schepers, D., Simmons, A., Soci, C., Abdalla, S., Abellan, X., Balsamo, G., Bechtold, P., Biavati, G., Bidlot, J., Bonavita, M., De Chiara, G., Dahlgren, P., Dee, D., Diamantakis, M., Dragani, R., Flemming, J., Forbes, R., Fuentes, M.A., Geer, A., Haimberger, L., Healy, S., Hogan, R. J., Holm, E., Janiskova, M., Keeley, S., Laloyaux, P., Lopez, P., Lupu, C., Radnoti, G., de Rosnay, P., Rozum, I., Vamborg, F., Villaume, S., and Thepaut, J.-N.: The ERA5 global reanalysis, Quart. J. Roy. Meteorol. Soc., 146, 1999–2049, https://doi.org/10.1002/qj.3803, 2020.

Hitchman, M. H., Yoden, S., Haynes, P. H., Kumar, V., and Tegtmeier, S.: An observational history of the direct influence of the stratospheric Qquasi-biennial Ooscillation on the tropical and subtropical upper troposphere and lower stratosphere, J. Meteorol. Soc. Japan. Ser. II, 99, 239–267, https://doi.org/10.2151/jmsj.2021-012, 2021.

Holm, S.: A simple sequentially rejective multiple test procedure, Scand. J. Statist., 6, 65–70. https://www.jstor.org/stable/4615733, 1979.

Holton, J. R., and Lindzen, R. S.: An updated theory for the quasi-biennial cycle of the tropical stratosphere, J. Atmos. Sci., 29, 1076–1080, https://doi.org/10.1175/1520-0469(1972)029<1076:AUTFTQ>2.0.CO;2, 1972.

Holton, J. R., and Tan, H.-C.: The influence of the equatorial quasi-biennial oscillation on the global circulation at 50 mb, J. Atmos. Sci., 37, 2200–2208, https://doi.org/10.1175/1520-0469(1980)037<2200:TIOTEQ>2.0.CO;2, 1980.

Holton, J. R., and Tan, H.-C.: The quasi-biennial oscillation in the Northern Hemisphere lower stratosphere, J. Meteorol. Soc. Japan, Ser. II, 60, 140–148, https://doi.org/10.2151/jmsj1965.60.1_140, 1982.

Iza, M., Calvo, N., and Manzini, E.: The stratospheric pathway of La Niña, J. Clim., 29, 8899–8914, https://doi.org/10.1175/JCLI-D-16-0230.1, 2016.

Kawatani, Y., Hamilton, K., Watanabe, S., Anstey, J. A., Richter, J. H., Butchart, N., Orbe, C., Osprey, S. M., Naoe, H., Elsbury, D., Chen, C.-C., Garcia-Serrano, J., Glanville, A., Kerzenmacher, T., Lott, F., Palmerio, F. M., Park, M., Serva, F., Taguchi, M., Versick, S., and Yoshioda, K.: QBOi El Niño Southern Oscillation experiments: Overview of experiment design and ENSO modulation of the QBO, EGUsphere [preprint], https://doi.org/10.5194/egusphere-2024-3270, Weather and Clim.ate Dyn.amics, accepted, 2025.

Kumar, V., Yoden, S., and Hitchman, M. H.: QBO and ENSO effects on the mean meridional circulation, polar vortex, subtropical westerly jets, and wave patterns during boreal winter, J. Geophys. Res., 127, e2022JD036691. https://doi.org/10.1029/2022JD036691, 2022.

Liess, S., and Geller, M. A.: On the relationship between QBO and distribution of tropical deep convection, J. Geophys. Res., 117, https://doi.org~~wiley.com~~/10.1029/2011JD016317, 2012.

Lindzen, R. S., and Holton, J. R.: A theory of the quasi-biennial oscillation, J. Atmos. Sci., 25, 1095-1107, https://doi.org/10.1175/1520-0469(1968)025<1095:ATOTQB>2.0.CO;2, 1968.

Lopez-Parages, J., Rodriguez-Fonseca, B., Mohino, E., and Losada, T.: Multidecadal modulation of ENSO teleconnection with Europe in late winter: Analysis of CMIP5 models, J. Clim., 29, 8067–8081. https://doi.org10.1175/JCLI-D-15-0596.1, 2016.

Lott, F., Rani, R., McLandress, C., Podglaj~~g~~en, A., Bushell, A., Bramberger, M., Lee, H.-K., Alexander, J., Anstey, J., Chun, H.-Y., Hertzog, A., Butchart, N., Kim, Y.-H., Kawatani, Y., Legras, B., Manzini, E., Naoe, H., Osprey, S., Plougonven, R., Pohlmann, H., Richter, J. H., Scinocca, J., García-Serrano, J., Serva, F., Stockdale, T., Versick, S. Watanabe, S., and Yoshida, K.: Comparison between non-orographic gravity-wave parameterizations used in QBOi models and Strateole 2 constant-level balloons,~~.~~ Q~~uart~~. J. R~~oy~~. Meteorol. Soc., 150, 1–16, https://doi.org/10.1002/qj.4793, 2024.

Lu, H., Hitchman, M., Gray, L., Anstey, J., and Osprey, S.: On the role of Rossby wave breaking in the quasi-biennial modulation of the stratospheric polar vortex during boreal winter,~~,~~ Q. J. R. Meteorol. Soc., 146, 1939–1959, https://doi.org/10.1002/qj.3775, 2020.

Ma, T., Chen, W., An, X., Garfinkel, C. I., and Cai, Q.: Nonlinear effects of the stratospheric ~~Q~~quasi-~~B~~biennial ~~O~~oscillation and ENSO on the North Atlantic winter atmospheric circulation, J. Geophys. Res., 128, e2023JD039537, https://doi.org/10.1029/2023JD039537, 2023.

Marshall, A. G., Hendon, H. H., Son, S.-W., and Lim, Y.: Impact of the quasi-biennial oscillation on predictability of the Madden–Julian oscillation, Clim. Dyn., 49, 1365–1377, https://doi.org/10.1007/s00382-016-3392-0, 2017.

Martin, Z., Son, S.-W., Butler, A., Hendon, H., Kim, H., Sobel, A., Yoden, S., and Zhang, C.: The influence of the quasi-biennial oscillation on the Madden–Julian oscillation, Nat. Rev. Earth Environ., 2, 477–489, https://doi.org/10.1038~~www.nature.com/articles~~/s43017-021-00173-9, 2021.

Naoe, H., Kobayashi, C., Kobayashi, S., Kosaka, Y., and Shibata, K.: Representation of ~~Q~~quasi-~~B~~biennial ~~O~~oscillation in JRA-3Q, J. Meteorol. Soc. Japan, 103, 233–255~~(EOR)~~, https://doi.org/10.2151/jmsj.2025-012, 2025.

Naoe, H., and Shibata, K.: Equatorial quasi-biennial oscillation influence on northern winter extratropical circulation, J. Geophys. Res., 115, D19102, https://doi.org/~~doi:~~10.1029/2009JD012952, 2010.

Naoe, H., and Yoshida, K.: Influence of quasi-biennial oscillation on the boreal winter extratropical stratosphere in QBOi experiments, Q. J. R. Meteorol. Soc., 145, 2755–~~-~~2771, https://doi.org/10.1002/qj.3591, 2019.

Norris, J., Hall, A., Neelin, J. D., Thackeray, C. W., and Chen, D.: Evaluation of the tail of the probability distribution of daily and subdaily precipitation in CMIP6 models, J. Clim., 34, 2701–2721, https://doi.org/10.1175/JCLI-D-20-0837.1, 2021.

Oueslati, B., and Bellon, G.: Convective entrainment and large-scale organization of tropical precipitation: Sensitivity of the CNRM-CM5 hierarchy of models, J. Clim., 26, 2931–2946, https://doi.org/10.1175/JCLI-D-12-00314.1, 2013.

Pahlavan, H. A., Fu, Q., Wallace, J. M., and Kiladis, G. N.: Revisiting the quasi-biennial oscillation as seen in ERA5. Part I: Description and momentum budget, J. Atmos. Sci., 78, 673–691, https://doi.org/10.1175/JAS-D-20-0207.1, 2021.

Palmeiro, F. M., García-Serrano, J., Ruggieri, P., Battée, L., and Gualdi, S.: On the influence of ENSO on sudden stratospheric warmings, J. Geophys. Res., 128, e2022JD037607, https://doi.org/10.1029/2022JD037607, 2023.

Palmeiro, F., Iza, M., Barriopedro, D., Calvo, N., and Garcia-Herrera, R.: The complex behavior of El Niño winter 2015–2016. Geophys. Res. Lett., 44, 2902–2910. https://doi.org/10.1002/2017GL072920, 2017.

Park, C.-H., Son, S.-W., Lim, Y., and Choi, J.: Quasi-biennial oscillation-related surface air temperature change over the western North Pacific in late winter, Int. J. Climatol., 30, 4351–4359, https://doi.org/10.1002/joc.7470, 2022.

Park, C.-H., and Son, S.-W.: Relationship between the QBO and surface air temperature in the Korean Peninsula, Atmosphere (Korean Meteor. Soc.), 32, 39–49, (in Korean), https://doi.org/10.14191/Atmos.2022.32.1, 2022.

Plumb, R. A., and McEwan, A. D.: The instability of a forced standing wave in a viscous stratified fluid: A laboratory analogue of the quasi-biennial oscillation, J. Atmos. Sci., 35, 1827–1839, https://doi.org/10.1175/1520-0469(1978)035<1827:TIOAFS>2.0.CO;2, 1978.

Randall, D. A., Tziperman, E., Branson, M. D., Richter, J. H., and Kang, W.: The QBO-MJO connection: A possible role for the SST and ENSO, J. Clim., 36, 6515–6531, https://doi.org/10.1175/JCLI-D-23-0031.1, 2023.

Rao, J., Garfinkel, C. I., and White, I. P.: Impact of the quasi-biennial oscillation on the northern winter stratospheric polar vortex in CMIP5/6 models, J. Clim., 33, 4787–4813, https://doi.org/10.1175/JCLI-D-19-0626.1, 2020a.

Rao, J., Garfinkel, C. I., and White, I. P.: How does the quasi-biennial oscillation affect the boreal winter tropospheric circulation in CMIP5/6 models?, J. Clim., 33, 8975–8996, https://doi.org/10.1175/JCLI-D-20-0024.1, 2020b.

Rao, J., and Ren, R.: A decomposition of ENSO's impacts on the northern winter stratosphere: Competing effect of SST forcing in the tropical Indian Ocean, Clim. Dyn., 46, 3689–3707, https://doi.org10.1007/s00382-015-2797-5, 2016a.

Rao, J., and Ren, R.: Asymmetry and nonlinearity of the influence of ENSO on the northern winter stratosphere: 1. Observations, J. Geophys. Res., 121, 9000–9016, https://doi.org10.1002/2015JD024520, 2016b.

Rao, J., and Ren, R.: Asymmetry and nonlinearity of the influence of ENSO on the northern winter stratosphere: 2. Model study with WACCM, J. Geophys. Res., 121, 9017–9032, https://doi.org10.1002/2015JD024520, 2016c.

Richter, J. H., Anstey, J. A., Butchart, N., Kawatani, Y., Meehl, G. A., Osprey, S., and Simpson, I. R.: Progress in simulating the quasi-biennial oscillation in CMIP models, J. Geophys. Res., 125, e2019JD032362, https://doi.org/10.1029/2019JD032362, 2020.

Richter, J. H., Butchart, N., Kawatani, Y., Bushell, A. C., Holt, L., Serva, F., Anstey, J., Simpson, I. R., Osprey, S., Hamilton, K., Braesicke, P., Cagnazzo, C., Chen, C.-C., Garcia, R. R., Gray, L. J., Kerzenmacher, T., Lott, F., McLandress, C., Naoe, H., Scinocca, J., Stockdale, T. N., Versick, S., Watanabe, S., Yoshida, K., and Yukimoto, S.: Response of the quasi-biennial oscillation to a warming climate in global climate models, Q. J. R. Meteorol. Soc., 148, 1490–1518, https://doi.org/10.1002/qj.3749, 2022.

Richter, J. H., Matthes, K., Calvo, N., and Gray, L. J.: Influence of the Quasi-Biennial Oscillation and El Niño–Southern Oscillation on the frequency of sudden stratospheric warmings, J. Geophys. Res., 116, D20111. https://doi.org10.1029/2011JD015757, 2011.

Rodrigo, M., García-Serrano, J., and Bladé, I.: Quasi-Biennial Oscillation influence on tropical convection and El Niño variability, Geophys. Res. Lett., 52, e2024GL112854, https://doi.org/10.1029/2024GL112854, 2025.

Ruzmaikin, A., Feynman, J., Jiang, X., and Yung, Y. L.: Extratropical signature of the quasi-biennial oscillation, J. Geophys. Res., 110, D11111, https://doi.org/10.1029/2004JD005382, 2005.

Scaife, A. A., Athanassiadou, M., Andrews, M., Arribas, A., Baldwin, M., Dunstone, N., Knight, J., MacLachlan, C., Manzini, E., Muller, W. A., Pohlmann, H., Smith, D., Stockdale, T., and Williams, A.: Predictability of the quasi-biennial oscillation and its northern winter teleconnection on seasonal to decadal timescales, Geophys. Res. Lett. 41, 1752–1758, https://doi.org/10.1029/2004JD005382, 2014.

Serva, F., Anstey, J. A., Bushell, A. C., Butchart, N., Cagnazzo, C., Gray, L., Kawatani, Y., Osprey, S. M., Richter, J. H., and Simpson, I. R.: The impact of the QBO on the region of the tropical tropopause in QBOi models: present-day simulations, Q. J. R. Meteorol. Soc., 148, 1945–1964, https://doi.org/10.1002/qj.4287, 2022.

~~Shibata, K., Naoe, H.: Decadal amplitude modulations of the stratospheric quasi-biennial oscillation, J. Meteorol. Soc. Japan, 100, 29–44, https://doi.org/10.2151/jmsj.2022-001, 2022.~~

Simpson, I. R., Blackburn, M., and Haigh, J. D.: The role of eddies in driving the tropospheric response to stratospheric heating perturbations, J. Atmos. Sci., 66, 1347–1365, https://doi.org/10.1175/2008JAS2758.1, 2009.

Son, S.-W., Lim, Y., Yoo, C., Hendon, H. H., and Kim, J.: Stratospheric control of the Madden-Julian oscillation, J. Clim., 30, 1909–1922, http://journals.ametsoc.org/doi/10.1175/JCLI574, 2017.

Song, K. and Son, S.-W.: Revisiting the ENSO–SSW relationship, J. Clim., 31, 2133–2143, https://doi.org/10.1175/JCLI-D-17-0078.1, 2018.

Taguchi, M.: Wave driving in the tropical lower stratosphere as simulated by WACCM. Part II: ENSO-induced changes for northern winter, J. Atmos. Sci., 67, 543–555. https://doi.org10.1175/2009JAS3144.1, 2010a.

Taguchi, M.: Observed connection of the stratospheric Quasi-Biennial Oscillation with El Nino–Southern Oscillation in radiosonde data, J. Geophys. Res., 115, D18120. https://doi.org10.1029/2010JD014325, 2010b.

Taguchi, M., and Hartmann, D. L.: Increased occurrence of stratospheric sudden warmings during El Niño simulated by WACCM, J. Clim., 19, 324–332, doi:10.1175/JCLI3655.1, 2006.

Tegtmeier, S., Anstey, J., Davis, S., Ivanciu, I., Jia, Y., McPhee, D., Kedzierski, R. P.: Zonal asymmetry of the QBO temperature signal in the tropical tropopause region. Geophy. Res. Lett., 47, e2020GL089533. https://doi.org/10.1029/2020GL089533, 2020.

Trascasa-Castro, P., Maycock, A. C., Yiu, Y. Y. S., and Fletcher, J. K.: On the linearity of the stratospheric and Euro-Atlantic sector response to ENSO, J. Clim., 32, 6607–6626, https://doi.org/10.1175/JCLI-D-18-0780.1, 2019.

Tyrrell, N. L., Koskentausta, J. M., and Karpechko, A. Y.: Sudden stratospheric warmings during El Niño and La Niña: sensitivity to atmospheric model biases, Weather Clim. Dynam., 3, 45–58, https://doi.org/10.5194/wcd-3-45-2022, 2022.

Van Loon, H., and Labitzke, K.: The Southern Oscillation. Part V: The anomalies in the lower stratosphere of the Northern Hemisphere in winter and a comparison with the Quasi-Biennial Oscillation, Mon. Weather Rev., 115, 357–369, https://doi.org/10.1175/1520-0493(1987)115<0357:TSOPVT>2.0.CO;2, 1987.

Walsh, A., Screen, J. A., Scaife, A. A., and Smith, D. M.: Non-linear response of the extratropics to tropical climate variability, Geophys. Res. Lett., 49, e2022GL100416, https://doi.org/10.1029/2022GL100416, 2022.

Wang, J., Kim, H.-M., and Chang, E. K. M.: Interannual modulation of Northern Hemisphere winter storm tracks by the QBO, Geophys. Res. Lett., 45, 2786–2794, http://doi.orgwiley.com/10.1002/484-2017GL076929, 2018.

Watson, P. A. G., and Gray, L. J.: How does the quasi-biennial oscillation affect the stratospheric polar vortex?, J. Atmos. Sci., 71, 391–409, https://doi.org/10.1175/JAS-D-13-096.1, 2014.

Wei, K., Chen, W., and Huang, R.: Association of tropical Pacific sea surface temperatures with the stratospheric Holton–-Tan oscillation in the Northern Hemisphere winter, Geophys. Res. Lett., 34, L16814, doi:10.1029/2007GL030478, 2007.

Weinberger, I., Garfinkel, C. I., White, I. P., Oman, L. D., Aquila, V., and Lim, Y.-K.: The salience of nonlinearities in the boreal winter response to ENSO: Arctic stratosphere and Europe, Clim. Dyn., 53, 4591–4610, https://doi.org/10.1007/s00382-019-04805-1, 2019.

White, I. P., Lu, H., Mitchell, N. J., and Phillips, T.: Dynamical response to the QBO in the nNorthern wWinter stratosphere: signatures in wave forcing and eddy fluxes of potential vorticity, J. Atmos. Sci., 72, 4487–4507, https://doi.org/10.1175/JAS-D-14-0358.1, 2015.

Yamazaki, K., Nakamura, T., Ukita, J., and Hoshi, K.: A tropospheric pathway of the stratospheric quasi-biennial oscillation (QBO) impact on the boreal winter polar vortex, Atmos. Chem. Phys., 20, 5111–5127, https://doi.org/10.5194/acp-20-5111-2020, 2020.

Yoo, C., and Son, S.-W.: Modulation of the boreal wintertime Madden–-Julian oOscillation by the stratospheric quasi-biennial oscillation, Geophys. Res. Lett., 43, 1392–-1398, https://doi.org/doi:10.1002/2016GL067762, 2016.

Yukimoto, S., Kawai, H., Koshiro, T., Oshima, N., Yoshida, K., Urakawa, S., Tsujino, H., Deushi, M., Tanaka, T. Y., Hosaka, M., Yabu, S., Yoshimura, H., Shindo, E., Mizuta, R., Obata, A., Adachi, Y., and Ishii, M.: The MRI Earth System Model version 2.0, MRI-ESM2.0: description and basic evaluation of the physical component, J. Meteorol. Soc. Japan, 97, 931–965, https://doi.org/10.2151/jmsj.2019-051, 2019.

Zhou, W., Leung, L. R., and Lu, J.: Linking large-scale double-ITCZ bias to local-scale drizzling bias in climate models, J. Clim.;, 35, 7965–7979, https://doi.org/10.1175/JCLI-D-22-0336.1, 2022.

◦

QBOi El Nino Southern Oscillation experiments: Teleconnections of the QBO

Naoe, Hiroaki[1], Jorge L. García-Franco[2], Chang-Hyun Park[3], Mario Rodrigo[4], Froila M. Palmeiro[4,5], Federico Serva[6], Masakazu Taguchi[7], Kohei Yoshida[1], James A. Anstey[8], Javier García-Serrano[4,9], Seok-Woo Son[3], Yoshio Kawatani[10], Neal Butchart[11], Kevin Hamilton[12], Chih-Chieh Chen[13], Anne Glanville[13], Tobias Kerzenmacher[14], François Lott[15], Clara Orbe[16], Scott Osprey[17], Mijeong Park[13], Jadwiga H. Richter[13], Stefan Versick[14], Shingo Watanabe[18,19]

Supplement figures

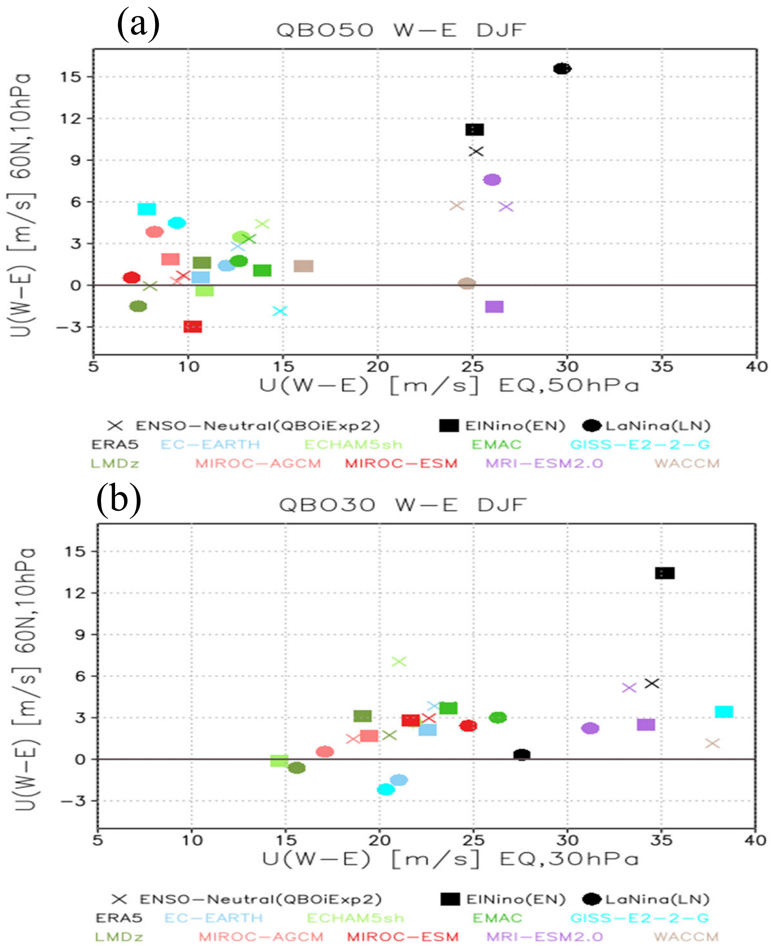

Figure S1: Relationship between~~of~~ QBO-W minus QBO-E composite differences in~~of~~ the zonal-mean zonal wind (in m s^{-1}) of~~between 10 hPa~~ polar vortex at 60° N and 10 hPa ~~and~~ QBO-W minus QBO-E differences in the zonal-mean zonal wind at the QBO definition region of~~at~~ (a) 50 hPa (QBO50~~, upper panel~~) and (b)~~at~~ 30 hPa (QBO30~~, lower panel~~). Crosses, filled squares, and filled circles indicate~~The~~ ENSO-neutral / ~~legend label indicates~~ QBOiExp2 (CTL), ~~the~~ El Niño / EN, and La Niña / LN winters in ERA5 or experiments in QBOi models, respectively~~ones indicate the EN and LN experiments~~.

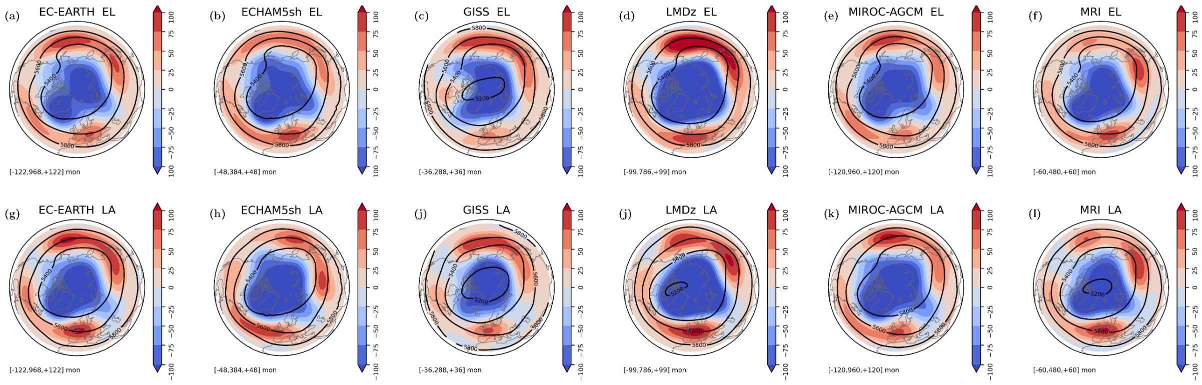

Figure S2: Northern annular mode (NAM) stereographic maps at 500 hPa forin EN and LN experiments infor the QBOi models, based on their daily geopotential heightdaily data (m). Contour lines indicate the geopotential height during neutral NAMannular mode conditions. Colors representare the positive (strong vortex, above the 90th percentile) minus negative (weak vortex, below the 10th percentile) year-around anomalies based on the NAM index. Negative anomalies indicate lower geopotential heights.

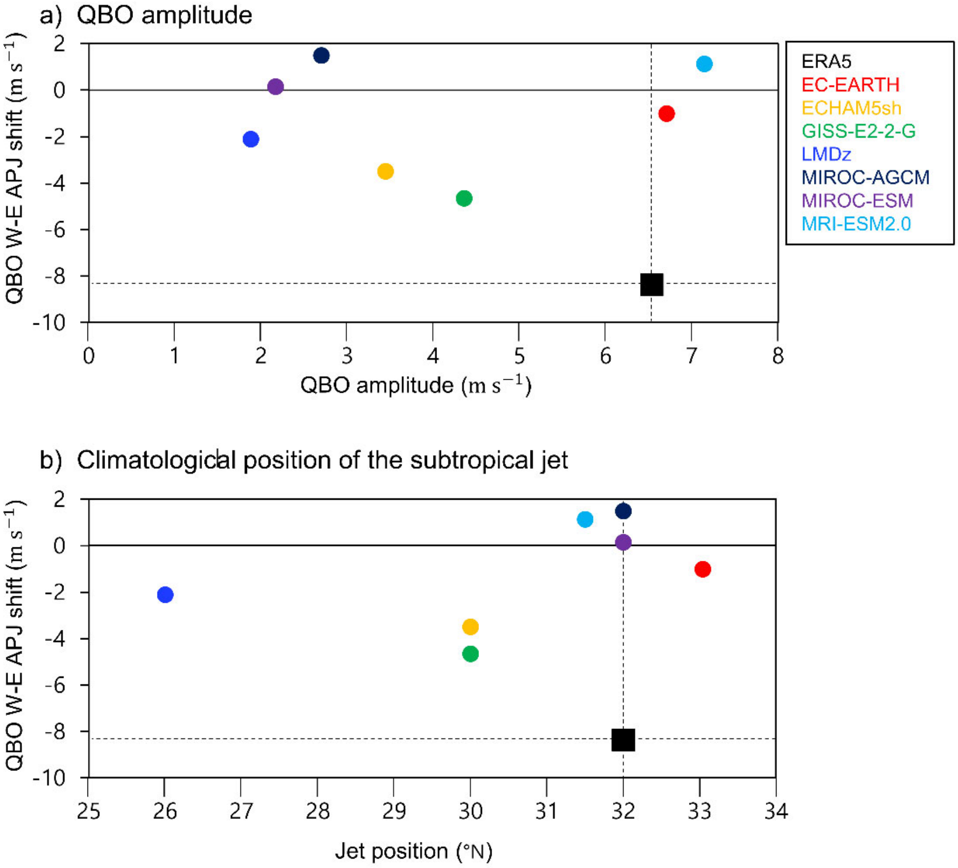

Fig. S3. Relationship between QBO-W minus QBO-E differences in the ~~QBO-induced~~ APJ shift index and (a) QBO amplitude, and (b) subtropical jet latitude for the CTL experiment / ~~during~~ ENSO-neutral ~~(CTL)~~ winters~~years~~.

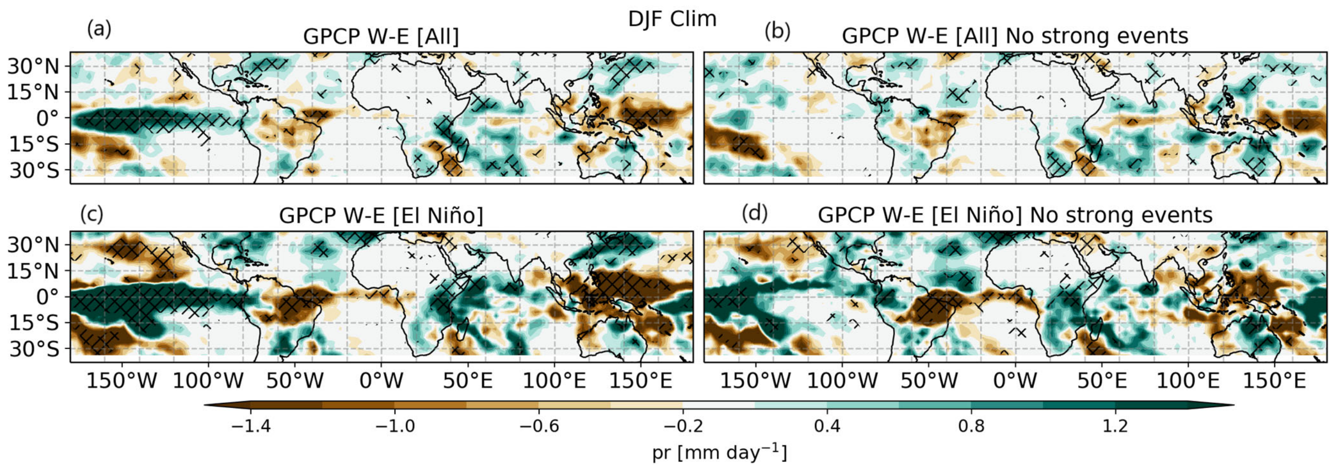

Figure S4. ~~DJF c~~Composite differences in GPCP (1979~~–~~–2021) precipitation (mm day^{-1}) during DJF between QBO-W and QBO-E phases ~~for W-E QBO phases~~, for~~considering~~ (top) all winters and (bottom) only El Niñ~~n~~o winters. ~~and~~ The ~~(~~left~~)~~ panels include~~ing~~ the three strongest El Niño events, while~~or~~ ~~(~~the right panels~~)~~ exclude~~removing~~ them.

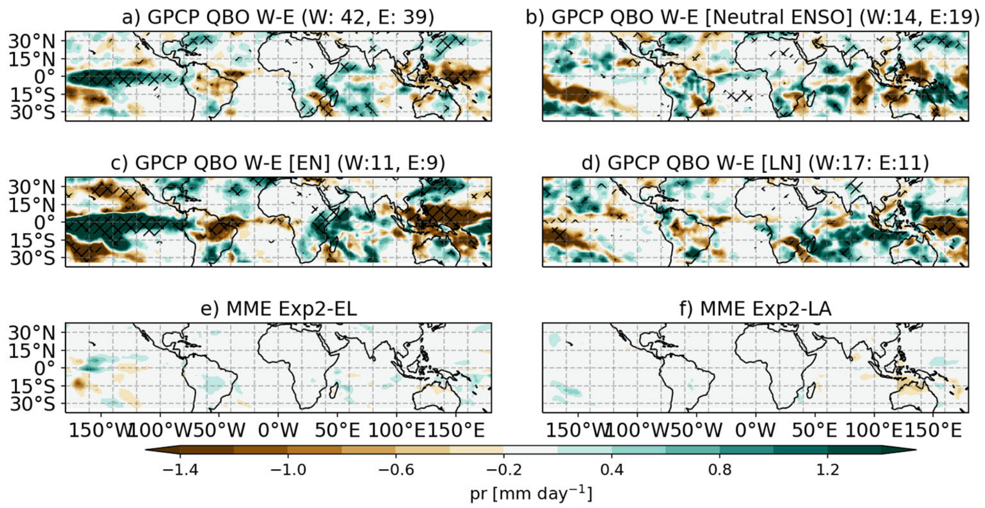

Figure S5. As in Figure 8, but showing ~~the~~ observed QBO signals (QBO-W minus QBO-W precipitation differences) during DJF for a) all ~~DJF~~ periods, ~~and under~~ b) ENSO-n~~N~~eutral, c) El Niño~~EN~~, and d) La Niña winters~~or LA conditions~~ based on GPCP data. ~~The~~ QBOi models are composited into a multi-model ~~-~~mean, regridded to ~~a common grid (~~the GPCP grid~~)~~, and a multi-model mean ensemble (MME) differences are shown for ~~the~~ e) EN and f) LN experiments. The degree of ~~M~~model agreement~~,~~ defined as grid ~~-~~points where at least 75% of ~~the~~ models agree on the sign of the signal~~,~~ is indicated by~~are~~ hatching~~ed~~. The number of months used for each observed composite ~~sizes in months~~ is~~are~~ shown in parenthes~~i~~es in the GPCP panels.

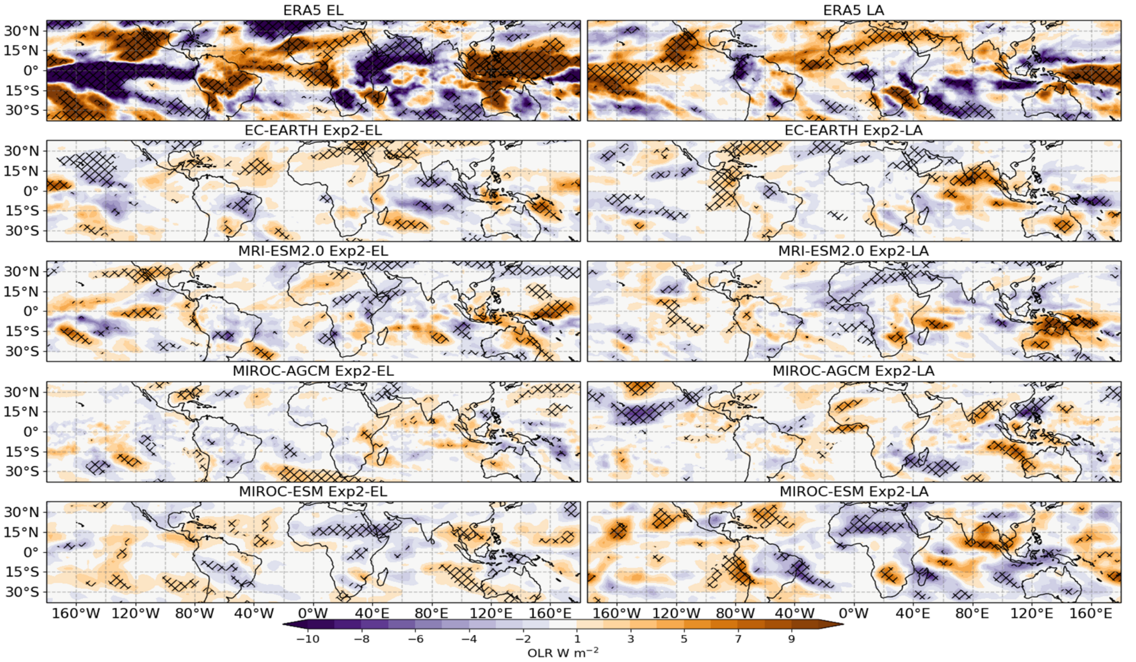

Figure S6: As Fig. 8, but for outgoing longwave radiation (OLR;) in W m^{-2}). ERA5 data are used as the observational benchmark. Only a subset ofsome models of the QBOi models providecohort OLR output OLR for these experiments.

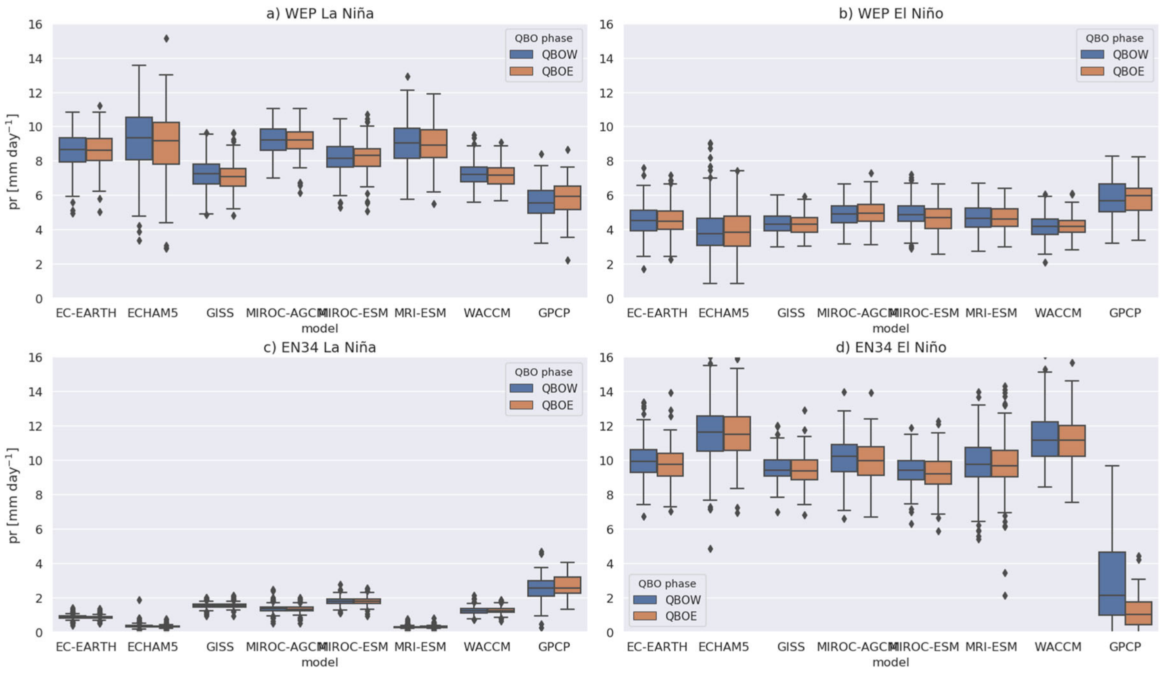

Figure S7: (Left) Box plots of deseasonalized precipitation (mm day^{-1}) ~~averaged over~~ for the western equatorial Pacific (WEP) region (5° S–5° N, 120°–170° E) and the EN3.4 region (5° S–5° N, 170°–120° W) for (a, c) LN and (b, d) EN experiments in~~for the~~ QBOi models, together with El Niño and La Niña winters~~years~~ in GPCP data, separated by dataset~~s~~ and QBO phase~~s~~. QBO phases are classified using deseasonalized DJF mean zonal-mean zonal wind at 50 hPa, averaged over 5° S–5° N, ~~at 50 hPa~~ with values~~using~~ ≥ 2 m s^{-1} indicating~~for~~ QBO-W and ≤ −2 m s^{-1} indicating~~for~~ QBO-E.

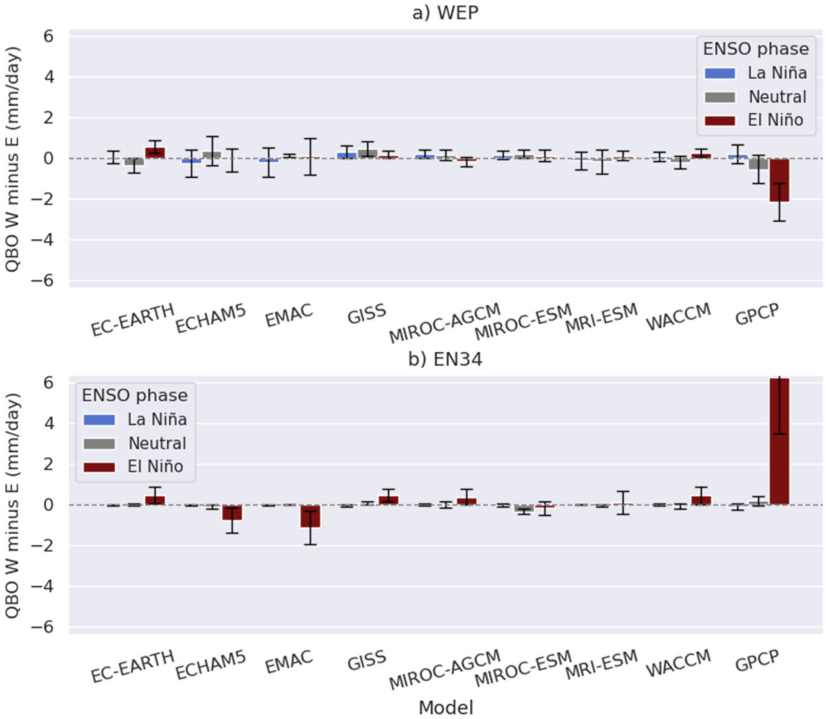

Figure S8: Same as Fig. 9, but withfor the y- axis limits are set according tobased on the GPCP scalebar.

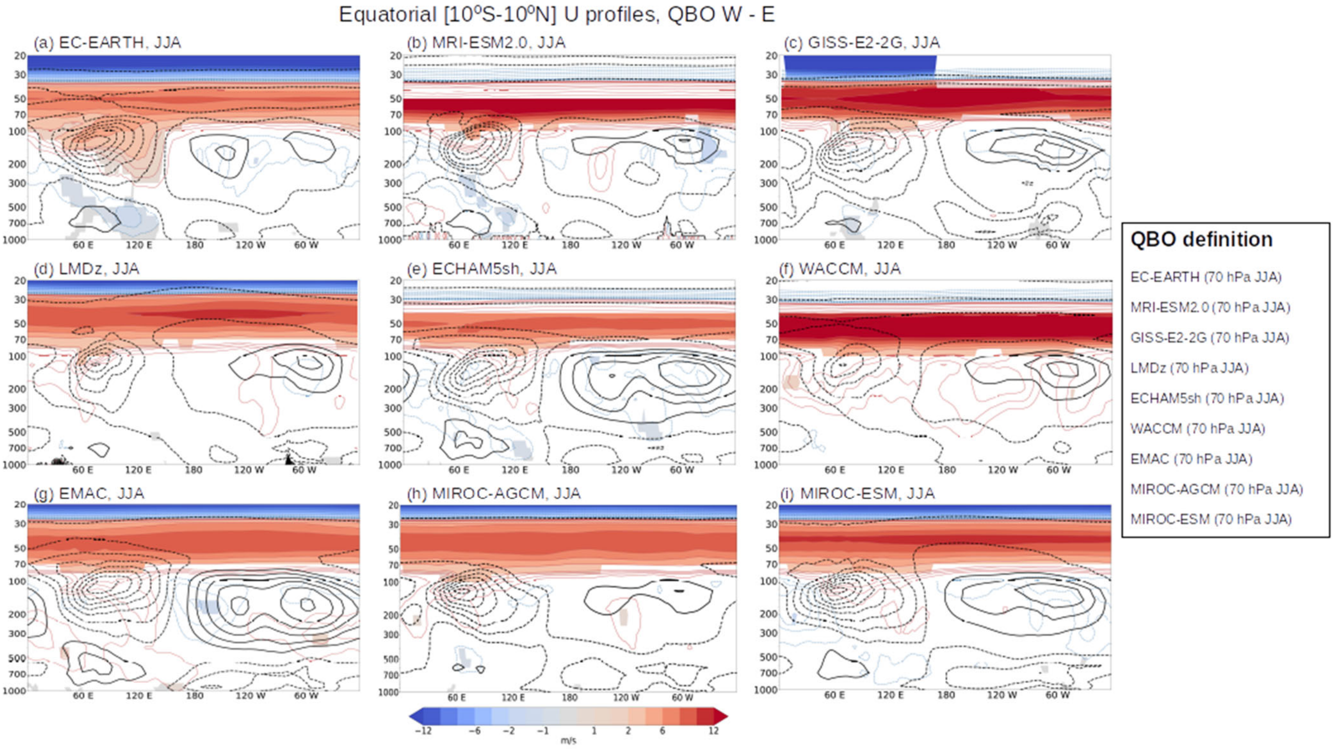

Figure S9: Climatology (black contours) and QBO-W minus QBO-E differences (shading and colored contours) in equatorial zonal wind (longitude–pressure section)~~profiles~~, averaged over 10° S–10° N, from the CTL experiment in~~for~~ the QBOi models. Black contours are drawn at 4 m s^{-1} intervals. Colored contours follow~~use~~ the same intervals as the shading, with red contours indicating positive differences and blue contours indicating negative differences. The target season is JJA for all models, with the QBO phase defined at 70 hPa during JJA. Only differences statistically significant ~~zonal wind differences~~ at the 95% confidence level are shaded.

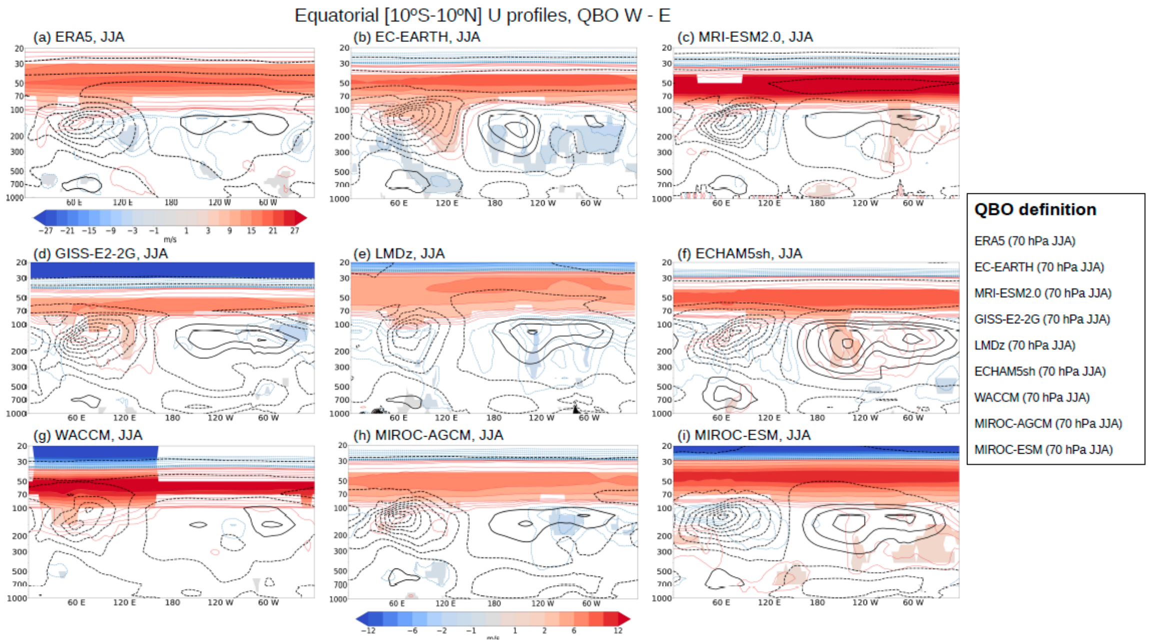

Figure S10: As in~~Same as~~ Fig.~~ure~~ S9, but for the LN experiment~~instead of CTL~~. Note that the ERA5 color scale~~bar~~ ~~for ERA5~~ differs due to~~because of~~ the larger QBO amplitude.

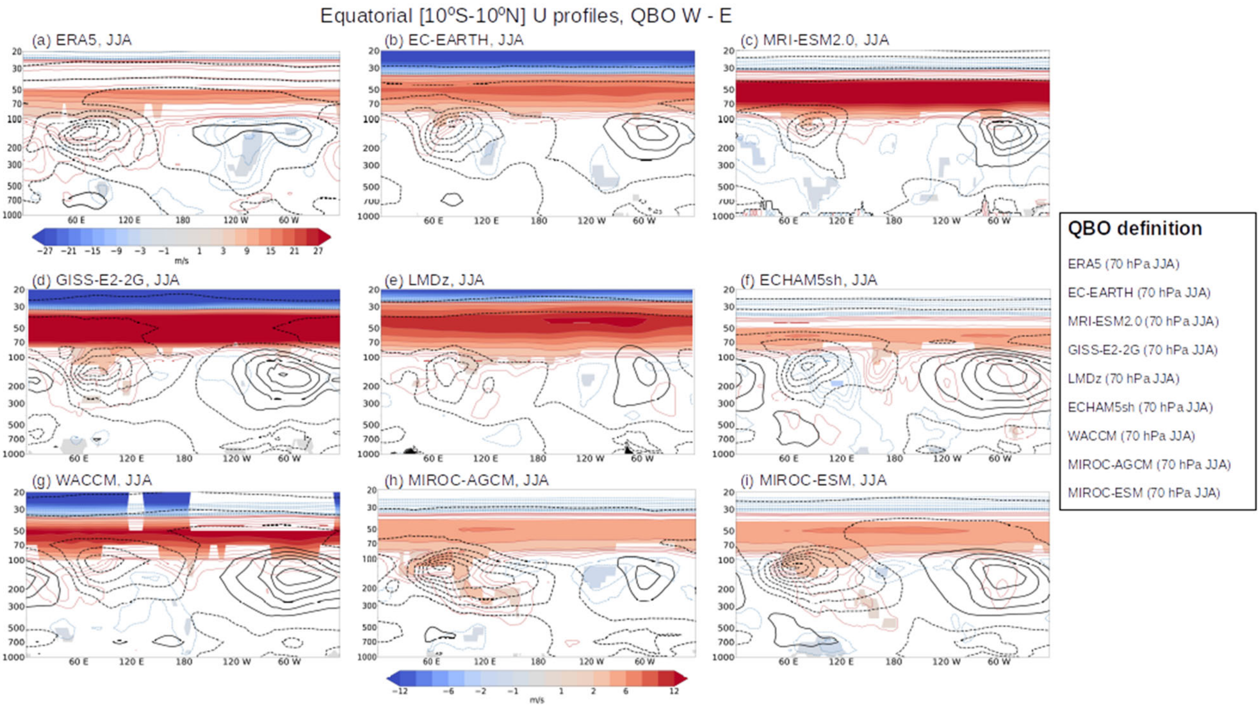

Figure S11: As in~~Same as~~ Fig.~~ure~~ S9, but for the EN experiment~~instead of CTL~~. Note that the ERA5 color scale~~bar~~ ~~for ERA5~~ differs due to~~because of~~ the larger QBO amplitude.

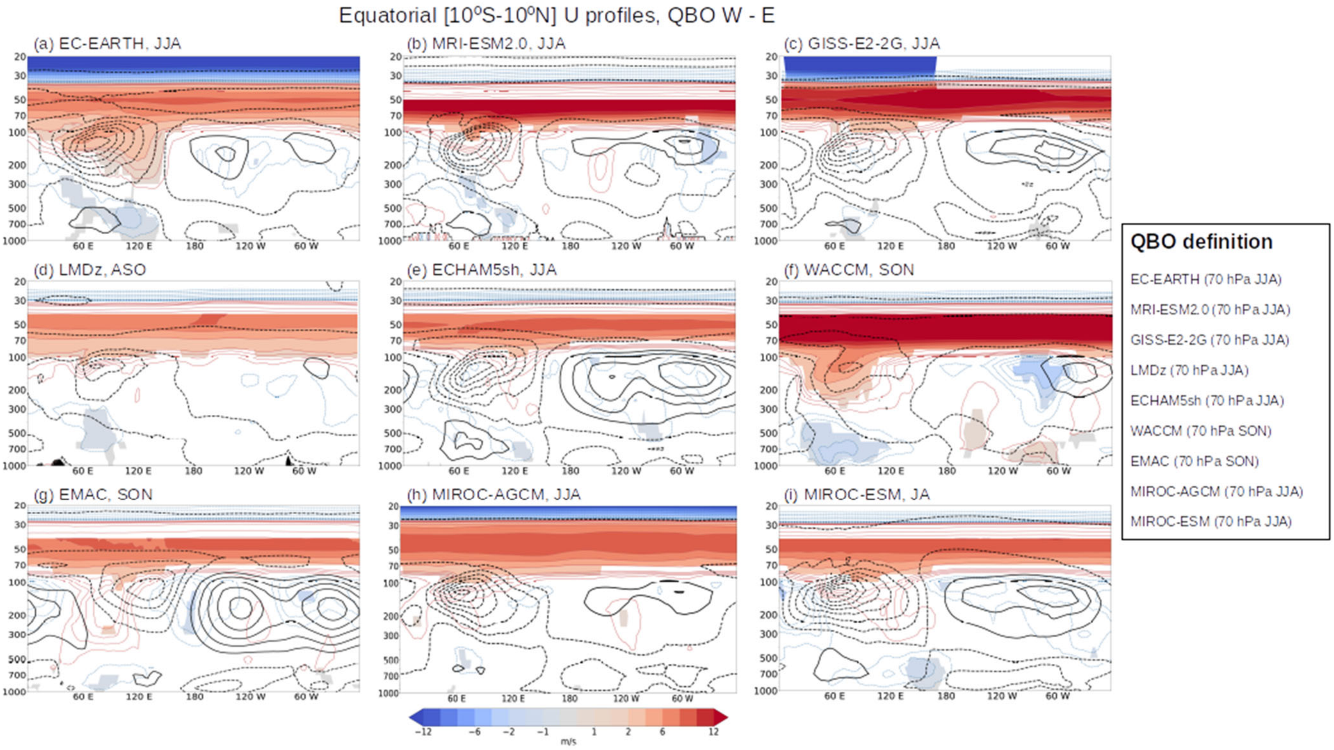

Figure S12: As in~~Same as~~ Fig.~~ure~~ 11, but for the CTL experiment~~s~~. ~~Note that t~~The EMAC model is used~~included~~ instead of ERA5, as~~because we have not considered~~ ENSO~~-~~-neutral years in the reanalysis are not considered.

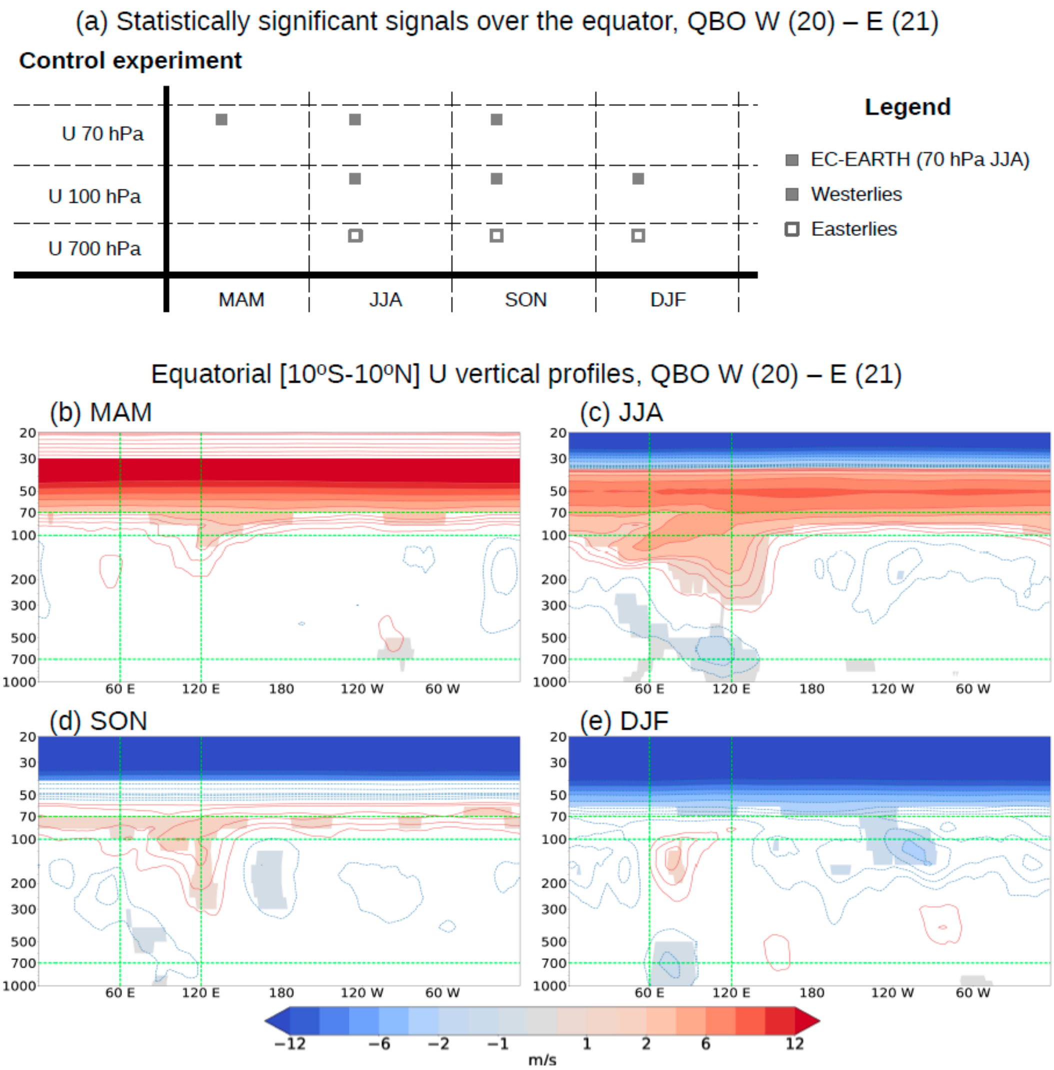

Figure S13: (a) Occurrence of ~~a~~ statistically significant zonal wind signals by season and altitude over the equatorial band (10° S–10° N,~~)~~ 60° E–120° E) ~~band~~ for the EC-EARTH CTL experiment ~~(a)~~. QBO-W minus QBO-E equatorial zonal wind (longitude–pressure section)~~profile~~ for the EC-EARTH CTL experiment during (b) MAM ~~(b)~~, (c) JJA ~~(c)~~, (d) SON ~~(d)~~, and (e) DJF ~~(e)~~. Horizontal green dashed lines denote ~~the~~representative vertical levels (700, 100, and 70 hPa), while vertical green dashed lines indicate~~mark~~ the longitudinal band (60° E–120° E) used in the season–altitude diagram (panel a).